UNCLASSIFIED

SE [illegible] OF THIS PAGE

(2)

	NTATION PAGE	Form Approved OMB No. 0704-0188 Exp. Date: Jun 30, 1985
1a	AD-A212 967 TE 1989	1b. RESTRICTIVE MARKINGS N/A Since Unclassified
2a	N/A Since Unclassified	3. DISTRIBUTION/AVAILABILITY OF REPORT Approved for public release; distribution unlimited.
2b. DECLASSIFICATION/DOWNGRADING SCHEDULE	N/A Since Unclassified	
4. PERFORMING ORGANIZATION REPORT NUMBER(S)	MRC-R-1240	5. MONITORING ORGANIZATION REPORT NUMBER(S) AFOSR-TR- 89-1234
6a. NAME OF PERFORMING ORGANIZATION	Mission Research Corporation	6b. OFFICE SYMBOL (If applicable)
7a. NAME OF MONITORING ORGANIZATION	Air Force Office of Scientific Research	
6c. ADDRESS (City, State, and ZIP code)	P.O. Drawer 719 735 State Street Santa Barbara, CA 93102	7b. ADDRESS (City, State, and ZIP code) Bolling Air Force Base Washington DC 20332-6448
8a. NAME OF FUNDING/SPONSORING ORGANIZATION	Same as 7a	8b. OFFICE SYMBOL (If applicable) NA
9. PROCUREMENT INSTRUMENT Identification NO.	F49620-86-C-0041	
8c. ADDRESS (City, State, and ZIP code)	Same as 7b	10. SOURCE OF FUNDING NUMBERS

PROGRAM ELEMENT NO.	PROJECT NO.	TASK NO.	WORK UNIT ACCESSION NO
61102F	2301	A8	

11. TITLE (Include Security Classification)
Time Evolution of the Electron Swarm Energy Distribution Function

12. PERSONAL AUTHOR(S)
N. J. Carron

13a. TYPE OF REPORT	13b. TIME COVERED	14. Date of Report (Year, Month, Day)	15. PAGE COUNT
Final	From Jun 86 to 30 Apr 89	89 June 28	32

16. SUPPLEMENTARY NOTATION

17. COSATI CODES			18. SUBJECT TERMS (continue on reverse if necessary and identify by block number)
FIELD	GROUP	SUB-GROUP	plasmas, Kinetic Theory, Distribution function, Energy Spectrum, Boltzman Equation, Swarm Theory

19. ABSTRACT (Continue on reverse if necessary and identify by block number)

The approximate theory of the Boltzmann Equation for the energy distribution function of swarm electrons is reviewed. The L, M approximation (essentially the Fokker-Planck approximation) is developed, being valid when average fractional energy loss per energy transfer collision is small, as is approximately the case in N_2 and O_2. A summary comparison with N_2 and O_2 swarm transport coefficients is presented showing excellent agreement over more than four orders of magnitude in the reduced electric field E/N_0.

We point out the importance of the spread of energy loss rate about the mean in determining the spectrum. The physical reason for the deficiency of the Continuous Slowing Down Approximation (CSDA) is clarified. It is further shown that the CSDA violates detailed balance. The classical distribution functions of Pidduck;

20. DISTRIBUTION AVAILABILITY OF ABSTRACT	21. ABSTRACT SECURITY CLASSIFICATION
☐ Unclassified/Unlimited ☒ Same as RPT. ☐ DTIC Users	UNCLASSIFIED

22a. NAME OF RESPONSIBLE INDIVIDUAL	22b. TELEPHONE (Include Area Code)	22c. OFFICE SYMBOL
Dr Robert Barker	202/767-5011	NP

DD FORM 1473, 84 MAR 83 Apr edition may be used until exhausted. SECURITY CLASSIFICATION THIS PAGE

All other editions are obsolete UNCLASSIFIED

Mission Research Corporation

/C.__/__/ MRC-R-1240

Time Evolution of the Electron Swarm Energy Distribution Function

N. J. Carron

June 28, 1989

[redacted] Technical Report

Contract No. F49620-86-C-0019

Prepared for: Air Force Office of Scientific Research
Bolling Air Force Base
Washington DC 20332-6448

Attention: Dr. Robert Barker
Program Manager

Prepared by: MISSION RESEARCH CORPORATION
735 State Street, P. O. Drawer 719
Santa Barbara, California 93102

19. ABSTRACT (Continued)

Druyvesteyn; Davydov; Morse, Allis, and Lamar; Chapman and Cowling; and Wannier are all special cases of a simple spectrum obtained in the L, M approximation. The physical meaning of its functional form is made clear by showing its relation to ordinary diffusion-convection theory.

The time dependent Boltzmann Equation in the L, M approximation is solved numerically for illustrative cases, demonstrating spectral time lag effects when the electric field varies on a time scale comparable with the swarm energy-transfer collision frequency.

TABLE OF CONTENTS

TABLE OF CONTENTS (CONCLUDED)

LIST OF ILLUSTRATIONS

LIST OF ILLUSTRATIONS (CONCLUDED)

SECTION 1

INTRODUCTION

This is the third in a series of reports[1, 2] documenting a useful, approximate solution of the Boltzmann Equation for the energy spectrum of swarm electrons (energy less than a few tens of eV) in a weakly ionized gas. We review the theory and then discuss time-dependent problems, extending the steady-state discussions of References 1 and 2.

The electrons are taken to suffer realistic momentum-transfer collisions (due to both elastic and inelastic scatterings), and inelastic energy-transfer collisions with the background host gas molecules. Requisite cross sections are taken from data. Electron-electron and electron-ion collisions are ignored compared to electron-neutral collisions. The gas molecules are in their own thermal equilibrium; rotational levels of diatomic molecules, for example, are thermally populated with a Maxwell-Boltzmann distribution at ambient temperature, and super-elastic collisions of electrons with excited states are included. We do not include thermally populated vibrational states because of unknown cross sections, although in principle they could easily be included.

An electric field $\vec{E}$ is present which causes the electrons to drift and to absorb energy from the field. It makes the distribution function non-isotropic. If the electric field is constant in time, the energy gained from it is lost to energy-transfer collisions at the same average rate, so the swarm will achieve a steady-state, which, however, is not a Maxwellian. The gas is considered an infinite energy sink.

Reference 1 presented the basic formulation, and introduced the usual mean Loss Function L, and the Straggling Function $\mathcal{M}$. It was shown that the energy spectrum, and most swarm transport coefficients, are determined to a good approximation by the momentum transfer cross section and two moments, L and $\mathcal{M}$, of the inelastic energy transfer cross sections. The spectrum is reduced to quadratures over these three molecular parameters. Reference 1 discussed the physical importance of straggling, obtained the differential equation for the time evolution of the energy spectrum in time varying fields, presented the expression for the steady state spectrum in a constant field, and applied it to N_2, comparing the spectrum itself with more detailed calculations, and comparing computed swarm parameters with data. Agreement with most swarm parameters is striking over some five orders of magnitude in the experimental parameter E/N_0. (N_0 is the molecular number density.) An exception is the

avalanche rate, which is rather larger than data at relatively small E/N_0. (Accurate agreement with the avalanche rate would not be expected.)

The form for the steady state spectrum is easily understandable in terms of ordinary diffusion-convection theory, being essentially a Fokker-Planck expansion in energy space, and requires small fractional mean energy loss per collision. Fractional energy loss is sufficiently small in N_2 and especially O_2 for the approximation to be valid over a useful wide span of E/N_0. Reference 1 also explained the physical reason for the inadequacy of the Continuous Slowing Down Approximation (CSDA) [in which, for example, the avalanche rate is orders of magnitude too small at relatively small E/N_0].

After a brief historical sketch, Reference 2 showed that the approximate steady state spectrum becomes exact in the limit that molecular quantum transition energies are small compared with the swarm energy and the gas temperature. The proof relies on detailed balance. This further shows that, in addition to the physical reasons for its inadequacy, the CSDA, which is commonly employed in analytic treatments, suffers the formal deficiency that it violates detailed balance. The steady state spectrum was then used to compute O_2 swarm parameters, and compared with data. Again the agreement is striking over some five orders of magnitude in E/N_0, with the avalanche rate again being an exception. In addition, an expression was presented for the energy spectrum in a sinusoidally time varying electric field. Finally, some more fundamental issues were raised concerning basic statistical mechanical approaches to the problem of determining the electron energy spectrum under the realistic random walk behavior in energy space.

Recommendations for some needed cross sections were made in References 3 and 4.

In the present report, we first review the basic theory in Section 2. Then in Section 3 we present a numerical finite difference algorithm for solving the differential equation previously derived as an approximation to the time-dependent integro-differential Boltzmann Equation. The remaining sections present various numerical solutions for time-evolving spectra.

SECTION 2

BASIC EQUATIONS AND REVIEW OF THEORY

In this section we briefly review the theory for the approximate Boltzmann Equation and its steady state solution. Details are in References 1 and 2.

2.1 THE BOLTZMANN EQUATION

Dropping spatial gradient terms, the Boltzmann Equation for the electron distribution function $f(\vec{v},t)$ in an electric field $\vec{E}$ and in a background gas is

$$\frac{\partial f}{\partial t} - \frac{e\vec{E}}{m} \cdot \nabla_v f = C + \text{Sources} - \text{Sinks} \qquad (1).$$

Here e is the magnitude of the electron charge. Actual sources and sinks are problem specific. They do not play a central role here, and will be dropped until a specific problem is considered. We concentrate on the effects of $\vec{E}$ and the collision integral C in determining f.

Many bulk plasma parameters depend only on the speed distribution function

$$F(v) = \int d\Omega_v f(\vec{v}) \qquad (2)$$

or, equivalently, on the energy spectrum g(w),

$$g(w) = \frac{v}{m} F(v) \qquad (3)$$

where $w = mv^2/2$ is the electron energy. If n is the electron number density, the normalizations are[5]

$$n = \int f(\vec{v}) d^3v = \int F(v) v^2 dv = \int g dw \qquad (4)$$

By suitable approximation to the collision integral, we shall obtain a differential equation for F or g. F will also be considered a function of w normalized to $\int F(w)\sqrt{w}dw = n$.

2.2 LEGENDRE EXPANSION FOR f

For reduced electric fields E/N_0 not too large, $V_{drift} \ll V_{thermal}$, and the departure from isotropy will be small. Then f is usefully developed in the usual Legendre Polynomial series in the angle θ between $\vec{v}$ and $\vec{E}$ [References 6,7].

$$\begin{aligned} f &= \sum_{\ell} f_\ell(v) P_\ell(\cos\theta) \\ &= f_0 + f_1 \cos\theta + \text{small terms} \end{aligned} \tag{5}$$

When electron-neutral collisions dominate, C is linear in f. C is also expanded, $C = C_0 + C_1 \cos\theta + \cdots$, and when the series is inserted in Eq. (5), the P_0 and P_1 parts become[6,7]

$$\frac{\partial f_0}{\partial t} - \frac{eE}{3m}\left(2\frac{f_1}{v} + \frac{\partial f_1}{\partial v}\right) = C_0 \tag{6a}$$

$$\frac{\partial f_1}{\partial t} - \frac{eE}{m}\frac{\partial f_0}{\partial v} = C_1 \quad . \tag{6b}$$

f_0 is essentially the energy spectrum, for

$$F(v) = \int (f_0 + f_1 \cos\theta) d\Omega_v = 4\pi f_0 \tag{7}$$

while f_1 controls bulk electron motion with drift velocity

$$\begin{aligned} \vec{v}_d &= \frac{1}{n}\int f\vec{v}d^3v = \frac{1}{n}\int (f_0 + f_1\cos\theta)\vec{v}d^3v \\ &= \frac{4\pi}{3n}\hat{E}\int f_1 v^3 dv \quad , \end{aligned} \tag{8}$$

where $\hat{E}$ is a unit vector in the direction of $\vec{E}$.

2.3 LEGENDRE EXPANSION OF COLLISION INTEGRAL

Thus C_0 is the collisional contribution to the time rate of change of the energy spectrum. It is discussed in Section 2.6 below.

C_1 is the contribution to the rate of change of that part of the spectrum that controls the swarm momentum. In general, for a weakly ionized gas in which electron-neutral collisions dominate[6,7], and when elastic collisions dominate the momentum transfer,

$$C_1 = -\nu_m f_1 \tag{9}$$

where $\nu_m = N_0 v \sigma_m$ is the mono-energetic momentum transfer collision frequency, σ_m is the momentum transfer cross-section, and N_0 is the background gas number density.

2.4 SLOWLY VARYING FIELDS

Equations (6) with (9) and a model for C_0 could be solved together forward in time to obtain the evolution of the distribution function, and so all transport coefficients. However a single equation can be obtained when fields vary slowly compared with ν_m. Inserting Eq. (9) into (6b),

$$\frac{\partial f_1}{\partial t} - \frac{eE}{m}\frac{\partial f_0}{\partial v} = -\nu_m f_1 \quad . \tag{10}$$

Thus, when $\partial/\partial t \ll \nu_m$, the first order distribution function is expressible in terms of the instantaneous energy spectrum without any time lag:

$$f_1 = \frac{eE}{m\nu_m}\frac{\partial f_0}{\partial v} \quad . \tag{11}$$

Since ν_m is generally greater than some 10^{11}sec^{-1} in sea level air, condition Eq. (11) holds in many circumstances.

The single equation for f_0 is now obtained by combining Eq. (11) with (6a). After a little algebra, it becomes

$$\frac{\partial f_0}{\partial t} - \frac{e^2E^2}{3m^2v^2}\frac{\partial}{\partial v}\left(\frac{v^2}{\nu_m}\frac{\partial f_0}{\partial v}\right) = C_0 \quad . \tag{12}$$

This may be written as well as an equation for g(w),

$$\frac{\partial g}{\partial t} + \frac{\partial}{\partial w}\left\{\frac{e^2E^2}{m\nu_m}\left[g - \frac{2}{3}\frac{\partial}{\partial w}(wg)\right]\right\} = C_g \tag{13}$$

where C_g is the collision integral for g. In this equation we have split the electric field contribution to the energy flux (curly brackets in Eq. (13)) into two parts, one proportional to g, and one to $\partial(wg)/\partial w$. Equation (13) exhibits the field's role in determining g.

2.5 ENERGY DIFFUSION IN THE ELECTRIC FIELD

The two parts correspond to a mean flux ($\sim$g), and a diffusive flux ($\sim \partial(wg)/\partial w$). As is well known, elastic scattering in the presence of an electric field produces both a mean gain in energy (rate $\sim e^2E^2/m\nu_m$), and a diffusion in energy (diffusion coefficient $\sim (2/3)we^2E^2/m\nu_m$). Diffusion is caused by scatterings parallel or anti-parallel to $\vec{E}$, spreading out the electrons' positions along the field, and therefore their potential energy.

That the diffusion term is important can be seen by comparing its effect in Eq. (13) to that of mean energy gain on a Maxwellian distribution of temperature T:

$$\frac{\text{Diffusive Gain Rate}}{\text{Mean Gain Rate}} = \frac{-\frac{2}{3}\frac{\partial}{\partial w}(wg)}{g} = -1 + \frac{2}{3}\frac{w}{T} \tag{14}$$

This is of order unity, and is therefore important. It changes sign over the average energy $3T/2$. The diffusion allows particles of energy $w > 3T/2$ to gain energy faster than the mean, and particles with $w < 3T/2$ to gain energy slower than mean, thus spreading out the spectrum.

2.6 THE INELASTIC COLLISION INTEGRAL

The general form for the collision integral is

$$C_g = \int g(w')P(w',w)dw' - g(w)\int P(w,w')dw' \tag{15}$$

where P(w,w')dw' is the probability per second that an electron with energy w collides and ends up with energy (w', w' + dw'). Inelastic collisional excitations to discrete molecular states k of energy w_k and cross section $\sigma_k(w)$ contribute to P an amount

$$P(w,w')dw' = N_0 v \sum_k \sigma_k \delta(w - w_k - w')dw' \tag{16}$$

assuming all host molecules in the ground state. (This assumption will be relaxed later. Rotational levels will be thermally populated.) Inserting this in Eq. (15) produces the usual expression,

$$C_g = N_0 \sum_k [(\sigma_k vg)_{w+w_k} - (\sigma_k vg)_w] \tag{17}$$

Since the cross sections are not exact step functions, the sum C_g itself is, of course, a continuous function of w. Developing the summand in a Taylor Series about w, we exhibit the first two terms,

$$C_g = N_0 \frac{\partial}{\partial w}\left[vgL + \frac{\partial}{\partial w}(vgM)\right] + \cdots \tag{18}$$

where

$$L = \sum_k w_k \sigma_k(w) \tag{19a}$$

$$M = \sum_k \frac{1}{2} w_k^2 \sigma_k(w) \tag{19b}$$

L is the Loss Function describing the mean energy loss rate to inelastic processes. M is a measure of the spread of energy loss rates about the mean. It is referred

to as the Straggling Function, and approximates the effects of the random walk in energy space. Energy loss to heavy particle recoil from elastic scatterings can easily be incorporated in the definitions. L and $\mathcal{M}$ are constructed from measured cross sections. The Continuous Slowing Down Approximation (CSDA) is that only the L term is retained.

Using Eq. (18), the equation for $\partial g/\partial t$ becomes

$$\frac{\partial g}{\partial t} + \frac{\partial}{\partial w}\left\{\frac{e^2E^2}{m\nu_m}\left[g - \frac{2}{3}\frac{\partial}{\partial w}(wg)\right]\right\} = N_0\frac{\partial}{\partial w}\left[vgL + \frac{\partial}{\partial w}(vg\mathcal{M})\right] \tag{20}$$

In flux conservative form,

$$\frac{\partial g}{\partial t} + \frac{\partial \phi}{\partial w} = 0 \ , \tag{21}$$

where

$$\phi = \frac{e^2E^2}{m\nu_m}\left[g - \frac{2}{3}\frac{\partial}{\partial w}(wg)\right] - N_0vgL - N_0\frac{\partial}{\partial w}(vg\mathcal{M}) \tag{22}$$

is the flux in energy space.

The effect of thermal motion of gas scatterers was discussed in [Reference 1], where it was shown that the Davydov term that usually accounts for it can be neglected if thermally populated rotational states are included.

2.7 SPREAD IN ENERGY LOSS

The ratio $\mathcal{M}/L$ is more slowly varying than L or $\mathcal{M}$ itself, since irregular behavior in the cross sections, such as the N_2 resonance spike near 2.5 eV, will occur in both L and $\mathcal{M}$ and divide out in the ratio.

Spread about the mean energy loss rate L can be compared with L. From Eq. (22) it is of order

$$\frac{\text{Diffusive Loss Rate}}{\text{Mean Loss Rate}} \sim \frac{1}{vgL}\frac{\partial}{\partial w}(vg\mathcal{M}) \sim \frac{\mathcal{M}}{\bar{w}L} \tag{23}$$

where $\bar{w}$ is the energy over which $\mathcal{M}g = (\mathcal{M}/L)Lg$ changes much, being of order the swarm temperature or a characteristic energy over which L itself changes. This ratio is not negligibly small, and can be of order unity (or larger, near thermal energies where L changes sign), showing that diffusive contributions to energy loss can be comparable to the mean loss, as was the case for energy gain in the electric field. Since in steady state mean loss essentially balances mean gain, diffusive loss can be as important as diffusive gain in determining the spectrum.

2.8 IMPORTANCE OF ENERGY DIFFUSION

The steady state spectrum is that for which $\phi = 0$, and results from a balance between total energy gain from E and total energy loss to collisions.

It is instructive to temporarily neglect the diffusive contributions to the flux; that is, the $\mathcal{M}$ term in the collision integral, and the term $-(2/3)\partial(wg)/\partial w$ in the electric field expression. The spectrum is then a balance between the mean rates.

The mean loss rate N_0vL increases with increasing energy, and the mean gain rate $e^2E^2/m\nu_m$ decreases with increasing energy. The rates cross and are equal at some energy w_1. An electron with energy $w > w_1$ loses energy faster than it gains it, and one with energy $w < w_1$ gains energy faster than it loses it. Consequently all electrons end up with energy w_1; the spectrum collapses to a delta function at the energy where the rates cross. Thus the physical process which actually determines the energy spectrum is spread in gain and loss rates about the mean. Mean rates determine only the average energy in the swarm. cf Figures 1a and 1b. It is clear that for electrons with a spread in energies to be in steady state there must be a balance between gain and loss rates over a spread in energies, and this spread determines the spectrum.

This shows that in the CSDA ($\mathcal{M} = 0$), the only physical process which establishes the spectrum, that is, gives body to the distribution function, is energy diffusion due to elastic scattering in the electric field, since in the collision integral only the mean loss rate is retained. The CSDA is poor because it neglects "half" of the physics determining the spectrum. We shall later show it also violates detailed balance.

Since energy diffusion is so important, we must keep the diffusive contribution in C_g as well to deduce a realistic spectrum. While L is the lowest order term in the expansion of C_g, $\mathcal{M}$ is the lowest order contributor to the energy distribution.

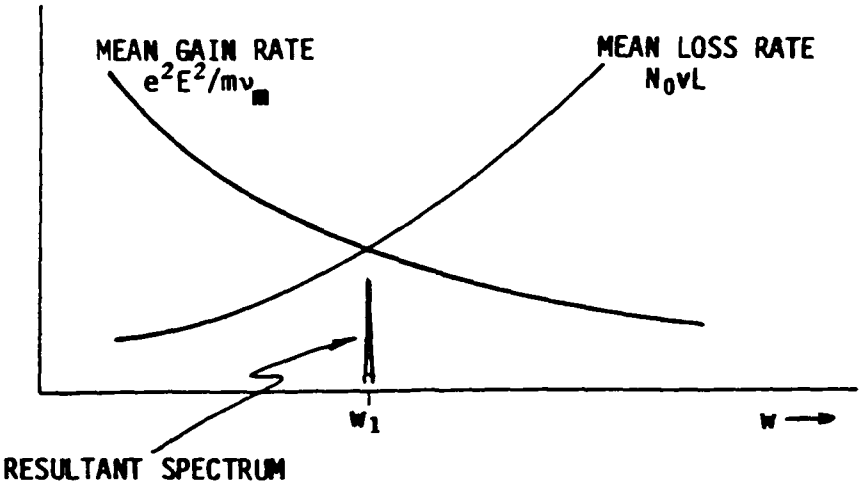

Figure 1a. Balance of mean gain and loss rates. Resultant spectrum is a δ function at w_1.

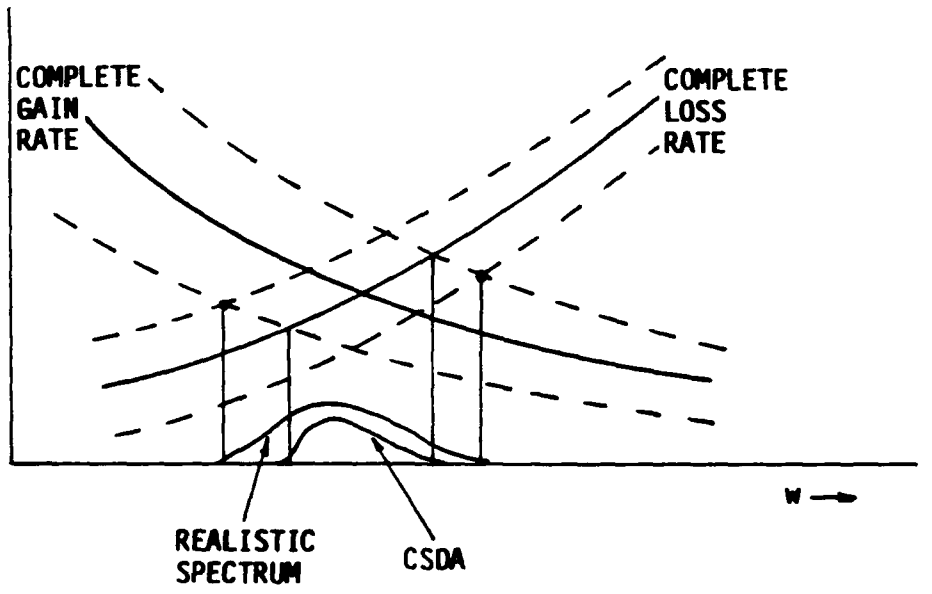

Figure 1b. Balance of complete gain and loss rates. CSDA neglects spread in energy loss.

From this point of view $\mathcal{M}$ should not be considered just another term in a Taylor Series expansion of a function. Rather it represents a critical piece of physics that must not be neglected. The functional form in which it appears is a Fokker-Planck approximation to the true random walk. The approximation is best when fractional energy loss per collision is small, and large energy changes occur only by a succession of small ones.

In particular, $\mathcal{M}$ allows some particles to lose energy slower than the mean, thereby supporting the high energy tail, and greatly increasing the avalanche rate or any process depending on the higher energy parts of the spectrum.

Conventional analytic treatments of the collision integral[6,7] retain only the mean energy loss, often expressing that due to inelastic processes as an adjustable multiple of that due to elastic processes. These treatments miss an important process contributing to the spectrum.

It is just as common for discrete losses due to, say, vibrational or electronic transitions, to not be included in a local differential analysis, it being believed their discrete nature precludes a differential treatment. Brief attention has been paid[8] to inelastic collision effects on the distribution function when molecular energy states are closely spaced, as for rotations of diatomic molecules, but a more general treatment such as that presented here seems not to have been pursued. The all important role played by spread of energy loss about the mean seems not to have been appreciated.

In fact, so long as average fractional energy loss per collision is small compared with unity, as is the case in N_2 and especially O_2 over wide energy ranges, a differential treatment including both L and $\mathcal{M}$ is justified, and its accuracy for calculating transport coefficients is borne out by direct calculation. This would almost certainly be true as well in many diatomic and polyatomic molecules.

2.9 ENERGY LOSS PER COLLISION

Electrons perform a random walk in energy space as they gain energy from E and lose it to inelastic collisions. The mean energy loss per energy- transfer collision is

$$w_\ell = \frac{L}{\sum_k \sigma_k} \tag{24}$$

The fractional energy loss $\xi = w_\ell/w$ in N_2 and O_2 at 300K is shown in Figure 2. ξ includes inelastic and super-elastic collisions with molecules in thermally

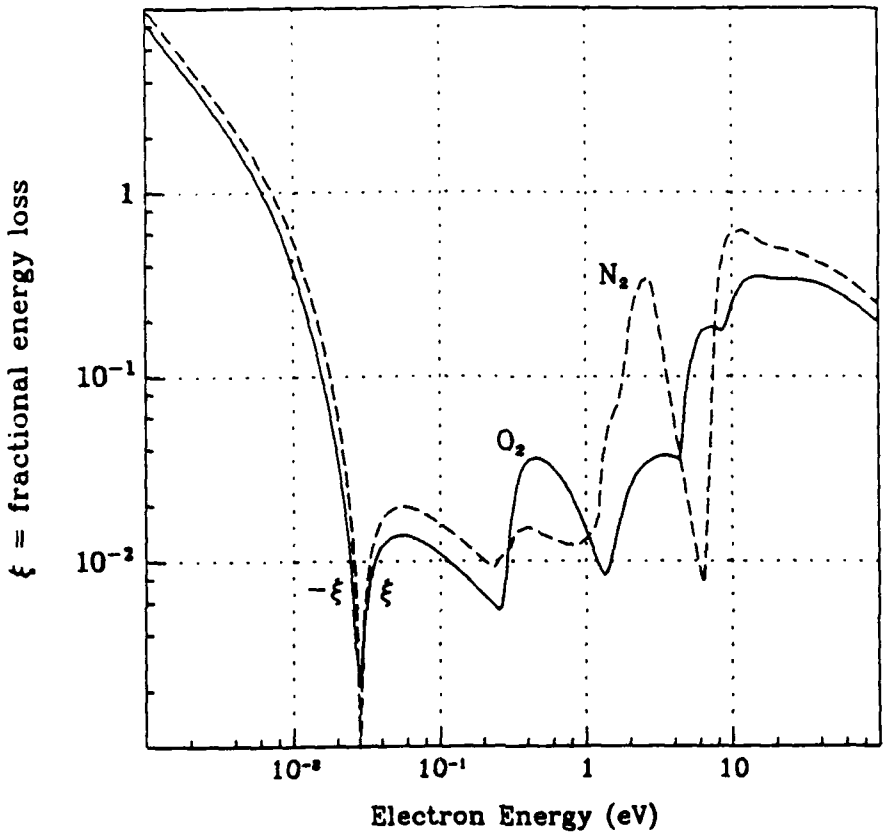

Figure 2. Fractional energy loss per energy transfer collision at 300K in N_2 and O_2.

populated rotational states. ξ is seen to be safely small except below about 0.01 eV, where rotational transitions with energies $4JB_0 \sim .01$ eV are common, and near 10 eV where high electronic excitations are most important. (Here $B_0 \sim 2 \times 10^{-4}$ eV is the rotational constant, and $J \sim 10$ is a typical populated rotational quantum number.) Except for these energy regions one would expect the Fokker-Planck approximation to be quite good.

Even at energies large enough for electronic excitation, which cause large single energy jumps, vibrational transitions still occur, reducing the average fractional energy loss. Figure 2 shows at 10 eV, say, that this appears to be more true for O_2 than N_2. Some computed swarm parameters will depart from experimental values

in N_2 when energy jumps due to electronic transitions are important in reducing the tail, or when the bulk of the spectrum spans the 2.5 eV resonance spike. Thus the characteristic energy will be computed to be too large when it is near 1 or 2 eV. Agreement is better in O_2.

2.10 EQUATION FOR TIME DEPENDENCE OF ENERGY SPECTRUM

Equation 20 controls the time evolution of the spectrum in time varying fields in the absence of sources and sinks:

$$\frac{\partial g}{\partial t} + \frac{\partial}{\partial w}\left\{\frac{e^2E^2}{m\nu_m}\left[g - \frac{2}{3}\frac{\partial}{\partial w}(wg)\right] - N_0 v L g - N_0 \frac{\partial}{\partial w}(v M g)\right\} = 0 \qquad (25)$$

Sources and sinks are to be added to the right hand side for a specific problem as appropriate. Eq. 25 is valid for E varying slowly compared with the momentum transfer frequency ν_m, but on any time scale relative to the mean energy transfer frequency. For example, following a pulsed ionization source this equation determines the relaxation of the spectrum toward equilibrium in the electric field and warm gas.

Clearly Equation 25, with vanishing right-hand side, preserves the normalization $n = \int g\,dw$. The swarm average energy

$$\bar{w} = \frac{1}{n}\int wg\,dw \qquad (26)$$

is then readily shown to obey

$$\frac{\partial \bar{w}}{\partial t} = -e\vec{E}\cdot\vec{v}_d - \frac{1}{n}\int dw\, N_0 v L g \qquad (27)$$

in the absence of sources and sinks. The swarm theory energy equation is obtained by introducing a swarm energy transfer collision frequency ν_w by

$$\frac{1}{n}\int dw\, N_0 v L g = \left(\bar{w} - \frac{3}{2}T\right)\nu_w \quad , \qquad (28)$$

where T is gas temperature, and using Eq. (28) to replace the last term in Equation (27). The direct contriubtion of $\mathcal{M}$ to $\partial\bar{w}/\partial t$ has dropped out. $\mathcal{M}$ still affects g and therefore the value of $\vec{v}_d$ and ν_w through their definitions in terms of the spectrum, and so indirectly alters $\partial\bar{w}/\partial t$.

For situations where E = 0, the equation resulting from Eq. (25),

$$\frac{\partial g}{\partial t} - N_0 \frac{\partial}{\partial w}\left\{ vLg + \frac{\partial(v\mathcal{M}g)}{\partial w} \right\} = 0 \quad , \tag{29}$$

determines the relaxation of g from an initial condition toward thermal equilibrium. Without the E term, Eq. 25 is no longer limited by $V_{drift} \ll V_{thermal}$ (two term Legendre series), and so applies to electrons of any energy. It includes mean energy loss, straggling, and thermal heating (through thermally populated rotational states in L and $\mathcal{M}$).

If straggling were to be neglected (CSDA), the resulting equation

$$\frac{\partial g}{\partial t} - N_0 \frac{\partial}{\partial w}(vLg) = 0 \qquad \text{(CSDA)} \tag{30}$$

would show simple convection in energy space, and therefore laminar flow. Electrons of higher energy would never overtake ones of lower energy. Straggling destroys laminar flow, and permits passing in energy space as actually occurs in a random walk.

Equation 25 can be written as well for F,

$$\frac{\partial F}{N_0 \partial t} - \frac{v}{w}\frac{\partial}{\partial w}\left\{ w\left[L + \frac{1}{w}\frac{\partial(w\mathcal{M})}{\partial w} \right] F + w\left[\frac{(eE/N_0)^2}{3\sigma_m} + \mathcal{M} \right] \frac{\partial F}{\partial w} \right\} = 0 \tag{31}$$

which will permit simpler understanding later.

2.11 STEADY STATE SPECTRUM

When $\partial/\partial t = 0$, the steady state solution of (31) is

$$F = F_0 \exp\left\{ - \int_0^w \frac{L + \frac{1}{w}\frac{\partial}{\partial w}(wM)}{\frac{(eE/N_0)^2}{3\sigma_m} + M} dw \right\} \tag{32}$$

where F_0 is a normalization constant. This is an improvement over the CSDA,

$$F = F_0 \exp\left\{ - \int_0^w \frac{3\sigma_m L}{(eE/N_0)^2} dw \right\} \tag{33}$$

which results when M is neglected.

The value of Eq. (32) lies both in its simplicity and (approximate) correctness, as well in its directly exhibiting the dependence of the distribution function on the most important molecular parameters σ_m, L, and M, and on the experimental parameter E. Scaling laws to other gases therefore become more transparent. Likewise, the dependence of transport coefficients, which are weighted integrals over F, on these parameters is also exhibited. Section 2.12 will further show the intuitive correctness of Eq. (32).

The Druyvesteyn spectrum is itself a special case of Eq. 33 for σ_m = constant, and elastic collisions only. In this case

$$L = \frac{2m}{M}\sigma_m w \quad . \tag{34}$$

Then F reduces to

$$F = F_0 \exp\left\{ - \frac{3m\sigma_m^2 w^2}{M(eE/N_0)^2} \right\} = F_D \tag{35}$$

In this case, the more correct Eq. (32) is essentially the same as Eq. (35) because, for elastic collisions, $M \sim \frac{1}{2}(2m/M)wL \ll wL$, and the M correction is negligible. Thus in this special case the improved spectrum does not mar already good agreement with data.

Later sections compute swarm parameters with the spectrum Eq. (32) for N_2 and O_2.

2.12 DIFFUSION-CONVECTION THEORY

The functional form for the steady state spectrum Eq. 32 is easily understood in terms of elementary diffusion and convection theory.

Let a quantity ψ diffuse and convect in one dimension x with diffusion coefficient D(x) and convection velocity V(x):

$$\frac{\partial \psi}{\partial t} + \frac{\partial}{\partial x}(V\psi) = \frac{\partial}{\partial x} D \frac{\partial \psi}{\partial x} \tag{36}$$

In steady state this equation shows that the flux must be constant in t and x:

$$V\psi - D\frac{\partial \psi}{\partial x} = \text{constant} = 0 \quad , \tag{37}$$

where the constant is taken to be 0 since we assume ψ and $\partial\psi/\partial x$ vanish at an end point. Then

$$\frac{1}{\psi}\frac{\partial \psi}{\partial x} = \frac{V}{D} \quad . \tag{38}$$

In steady state the convection velocity and diffusion coefficient determine the logarithmic derivative of ψ by Eq. 38. Consequently ψ is distributed according to

$$\psi = \psi_0 \exp\left\{\int \frac{V}{D} dx\right\} \tag{39}$$

If we now take x to be the electron energy w, and ψ the spectrum F, the flux in curly brackets in Equation (31) identifies

$$V = -N_0 v \left[L + \frac{1}{w}\frac{\partial}{\partial w}(wM)\right] \tag{40}$$

$$D = N_0 v \left[\frac{(eE/N_0)^2}{3\sigma_m} + M\right] \tag{41}$$

so that the solution Eq. 39 is the steady state spectrum Eq. 32.

- $N_0 vL$ is the prescribed convection velocity, and the $(1/w)\ \partial(wM)/\partial w$ term is the additional convection due to the energy dependence of the diffusion coefficient. Their sum is the total convection velocity. The first term in Eq. 41 is the diffusion coefficient due to elastic scattering in E, and the M term is that due to energy loss straggling. Their sum is the total diffusion coefficient.

The electric field E_D at which the two diffusion coefficients are equal is

$$\frac{eE_D}{N_0} = \sqrt{3\sigma_m M} \quad , \tag{42}$$

and is a function of w. In O_2 it is as small as 0.1 Td for $w \lesssim 0.1$ eV, about 1 Td near 0.3 eV, 10 Td at 4.0 eV, and greater than 100 Td for $w \gtrsim 9$ eV. In N_2 it is more widely variable because of the resonance spike which causes both σ_m and M to peak near 2.5 eV.

(The mean gain velocity $e^2E^2/m\nu_m$ and the velocity $-(2/3)e^2E^2/m\nu_m$ due to the energy dependence of the electric field diffusion coefficient would also appear directly if we had applied these ideas to Equation (25) for g. They drop out in the numerator of the final distribution function[1]).

2.13 EXACT LIMIT FOR SMALL QUANTUM TRANSITIONS

When $E = 0$, the spectrum Eq. 32 must reduce to a Maxwellian. Reference 2 derives explicitly the condition

$$\frac{L + \frac{1}{w}\frac{\partial}{\partial w}(wM)}{M} = \frac{1}{T} \tag{43}$$

that assures this. Here T is gas temperature. This condition is exactly true only for the limit of small molecular quantum transition energies; it is only approximately true for real cross sections and real L and M. Its derivation requires detailed balance, and uses the complete expression for L

$$L(w) \ = \ \sum_{i,k} N_i(E_k - E_i)\sigma_{ik}(w)$$

$$= A \sum_{i,k} D_i e^{-E_i/T} (E_k - E_i) \sigma_{ik}(w) \qquad (44)$$

that includes thermally populated excited states of energy E_i, and degeneracy D_i, and with electronic cross section $\sigma_{ik}(w)$ for transitions from i to k. An expression similar to Eq. 44 holds for $\mathcal{M}$. $N_i = AD_i e^{-E_i/T}$ is the population of the i-th level, where $A = N_0 / \sum_i D_i e^{-E_i/T}$.

When $|E_k - E_i| \ll T$ or w, then an expansion in the small ratios $|E_k - E_i|/T$ and $|E_k - E_i|/w$, together with detailed balance, leads to condition (Eq. 43). This condition is the necessary relation that must hold between the Fokker-Planck coefficients of friction and diffusion. In particular, the CSDA ($L \neq 0, \mathcal{M} = 0$) violates it and is therefore inconsistent with detailed balance.

Eq. 32 appears to be significantly superior to the CSDA, the fractional energy loss ξ being small enough so that the Fokker-Planck approximation is valid. When used to compute transport coefficients by integrating over the spectrum, a higher accuracy is achieved, and results are in surprisingly good agreement with data.

In this limit, using Eq. (43), one could eliminate L in Eq. (32) to obtain

$$F = F_0 \exp\left\{ -\frac{1}{T} \int_0^w \frac{1}{\frac{(eE/N_0)^2}{3\sigma_m \mathcal{M}} + 1} dw \right\} \qquad (45)$$

reducing the dependence on molecular and experimental quantities to the single parameter $(eE/N_0)^2/3\sigma_m \mathcal{M}$. This form is appealing in its simplicity, and is essentially the Chapman-Cowling result (discussed in Section 2.14) with LT replaced by $\mathcal{M}$. However, it focusses attention on the straggling function $\mathcal{M}$, and detracts from the more physically transparent form of Equations (32) and (39). We shall therefore work with the distribution function in the form of Equation (32).

2.14 PREVIOUS DISTRIBUTION FUNCTIONS AS SPECIAL CASES

We have already mentioned in Section 2.11 that the Druyvesteyn spectrum is a special case of the CSDA (for σ_m = constant), which is a special case of Equation (32). Other historically important distribution functions have been obtained by Pidduck[9]; Davydov[10]; Morse, Allis, and Lamar[11]; Chapman and Cowling[12]; and by Wannier[13]. All of these are intended to apply in the case of elastic collisions only. The later work

permits the momentum transfer cross section $\sigma_m(w)$ to be a function of energy, and accounts for thermal gas motion. We now show these are all approximate special cases of Equation (32).

Huxley and Crompton show that all formulae are included in that of Chapman and Cowling's, which in our notation is

$$F_{CC} = F_0 \exp\left\{ - \int_0^v \frac{mvdv}{\frac{M(eE/N_0)^2}{3(mv\sigma_m)^2} + T} \right\} \tag{46}$$

where T is gas temperature, and M is the molecular mass. Thus we need only show that this equation is contained in Equation (32).

For the conditions stated, L is

$$L = \frac{2m}{M} w \sigma_m(w) \tag{47}$$

and, using $mvdv = dw$, Equation (46) can then be written

$$F_{CC} = F_0 \exp\left\{ - \int_0^w \frac{Ldw}{\frac{(eE/N_0)^2}{3\sigma_m} + TL} \right\} \tag{48}$$

That this is a special case of Equation (32) may be seen by using Equation (43) to rewrite the $\mathcal{M}$ in the denominator of the integrand of Equation (32),

$$\mathcal{M} = TL + \frac{T}{w} \frac{\partial(w\mathcal{M})}{\partial w} \quad , \tag{49}$$

so that it becomes

$$F = F_0 \exp\left\{ - \int_0^w \frac{L + \frac{1}{w}\frac{\partial(w\mathcal{M})}{\partial w}}{\frac{(eE/N_0)^2}{3\sigma_m} + T\left(L + \frac{1}{w}\frac{\partial(w\mathcal{M})}{\partial w}\right)} dw \right\} \quad , \tag{50}$$

differing from Equation (48) only by the $(1/w)\partial(w\mathcal{M})/\partial w$ added to L. But for elastic collisions,

$$\mathcal{M} = \frac{1}{2}\frac{2m}{M} wL \quad , \tag{51}$$

and

$$\frac{1}{w}\frac{\partial}{\partial w}(w\mathcal{M}) = \frac{2m}{M} L \left[1 + \frac{w}{2L}\frac{\partial L}{\partial w}\right] \ll L \quad . \tag{52}$$

Therefore the $\mathcal{M}$ correction can be dropped, and the two expressions become the same.

For elastic collisions only, collisional energy transfers are indeed small compared with w and T, so we are justified in using Equation (43). Also for elastic collisions the $\mathcal{M}$ correction is small, allowing the above approximations.

When inelastic collisions contribute, as in vibrational excitations of diatomic molecules, the contribution $(1/w)\partial(w\mathcal{M})/\partial w$ to the convection velocity L, arising from the energy dependence of the diffusion coefficient, is not necessarily small, and can no longer be neglected. The distribution function in Equation (32) extends earlier theoretical expressions to the case of (small) inelastic collisions as well, and contains the earlier work as special cases.

2.15 STEADY STATE RESULTS FOR N_2

Earlier reports[1,3] collect requisite cross sections: momentum-transfer, rotational, vibrational, and electronic. Figure 3 shows L and $\mathcal{M}$ for N_2 at 300K constructed from them, including thermally populated rotational states and superelastic rotational collisions. The resonance spike near 2.5 eV and the high first electronic excitation (6.17 eV) make N_2 a particularly stressful case in which to test the Fokker-Planck Equation 32. In fact the spectrum computed in a field of 100 Td, Figure 4 [Reference 1],while superior to the CSDA, is not very close to more accurate published calculations[14]. ($1Td = 10^{-17} V - cm^2$). However transport coefficients are in much better agreement with data, except for those dependent on the tail.

Figure 5 shows the calculated drift velocity (open circles) with data compiled by Dutton[15] over some five decades in E/N_0. The agreement is excellent everywhere except between 10^{-16} and $10^{-15} Vcm^2$, where calculated drift velocities are some 20% low. At these field strengths, the characteristic energy is between 1 and 3 eV, and is computed to be too large (Figure 6) partly because of the high spectral tail, and

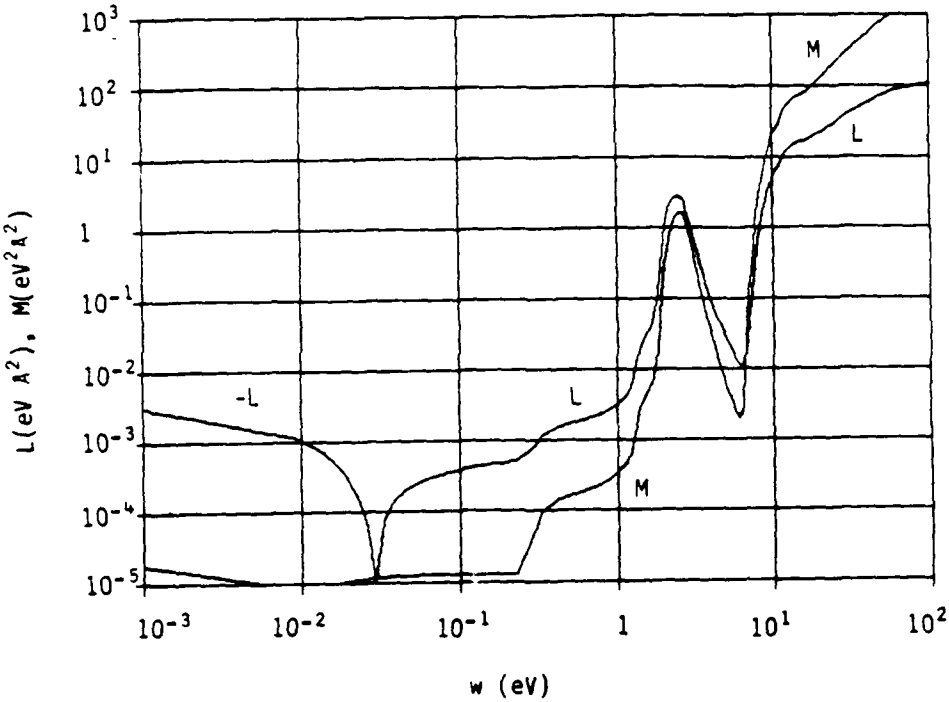

Figure 3. $\mathcal{M}$ and L functions for N_2 at 300 K.

partly because the spectrum straddles the resonance. At even higher fields the drift velocity returns to good agreement.

Figure 7 shows swarm momentum- and energy-transfer collision frequencies as a function of characteristic energy up to 1 eV, compared with more detailed calculations. Again the agreement is excellent except for the energy-transfer frequency at 1 eV.

Figure 8 shows the avalanche rate above 10^{-15}V $-$ cm^2. At relatively low E/N_0 it is computed to be more than an order of magnitude too large, due again to the high tail seen in Figure 4.

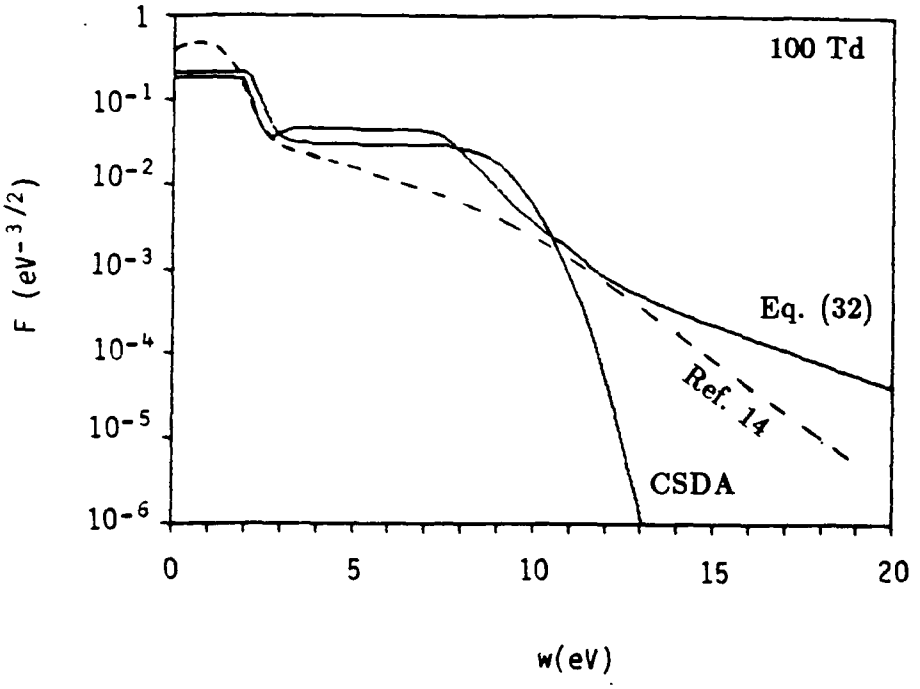

Figure 4. Energy spectrum at 10^{-15} V-cm^2 from Eq. (32), the CSDA, and Reference 14.

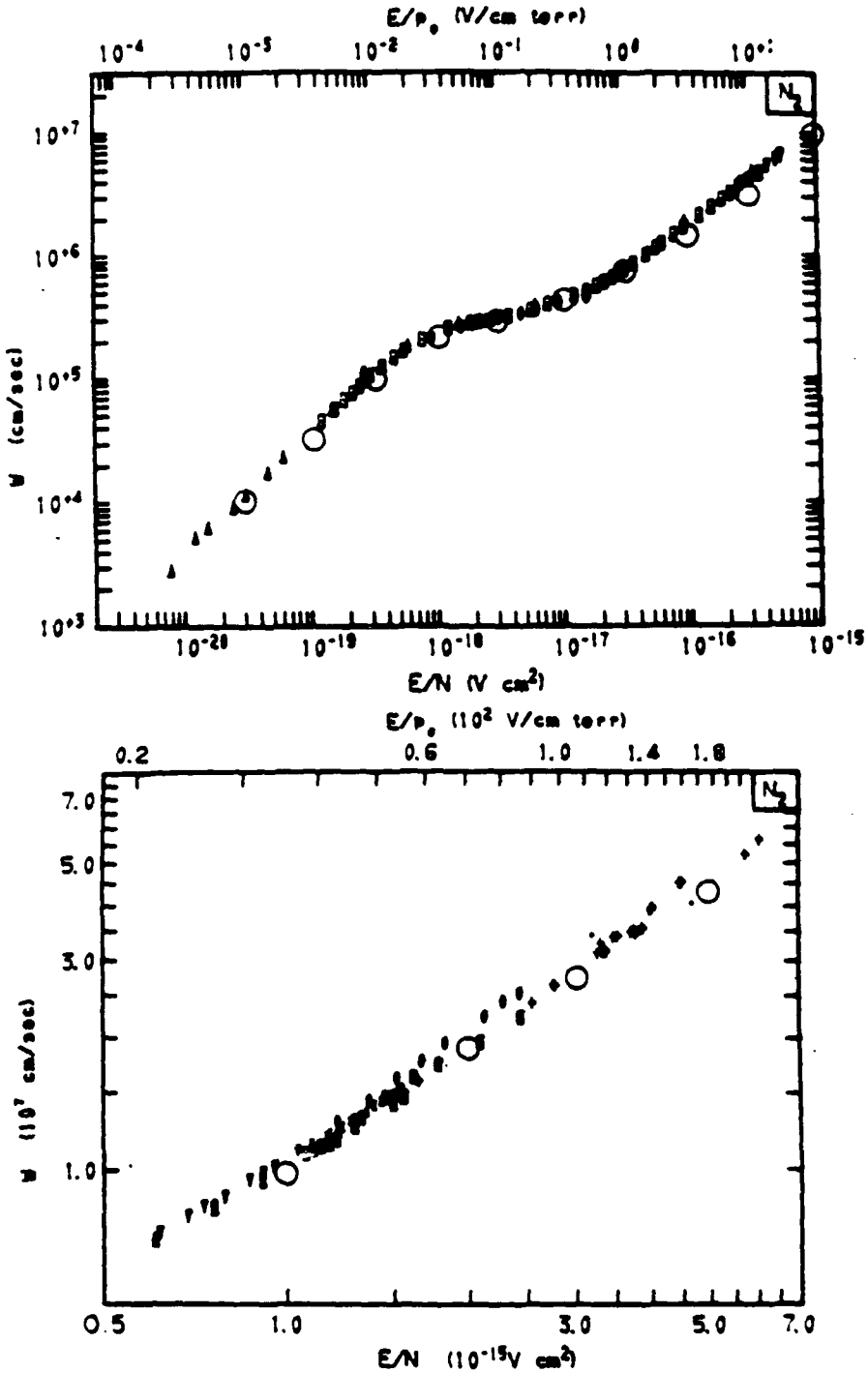

Figure 5. Calculated N_2 drift velocity (open circles) with data compiled by Dutton (Ref. 15).

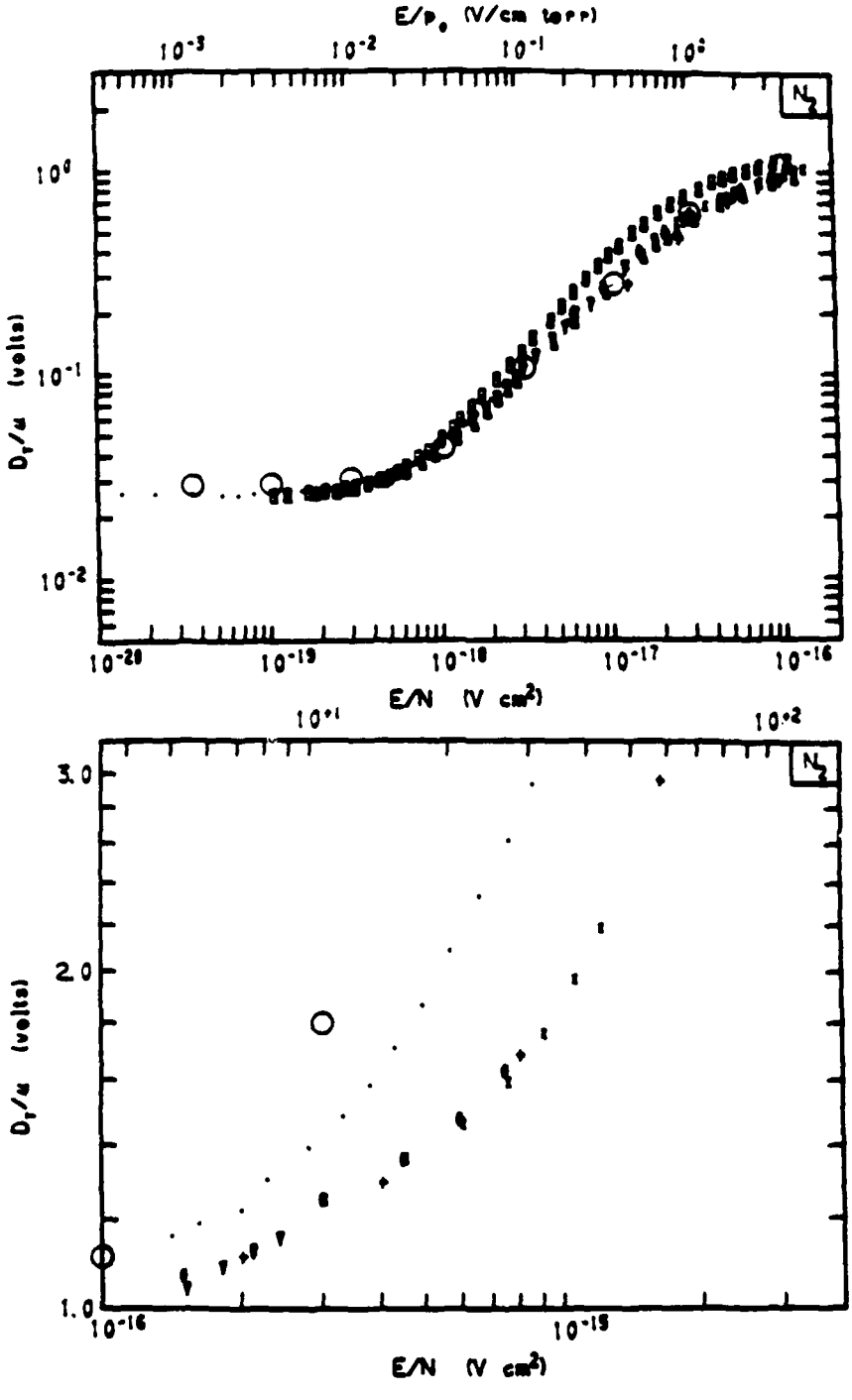

Figure 6. **Calculated swarm characteristic energies in N_2 (open circles) with data compiled by Dutton (Ref. 15). Ambient temperature (300 K).**

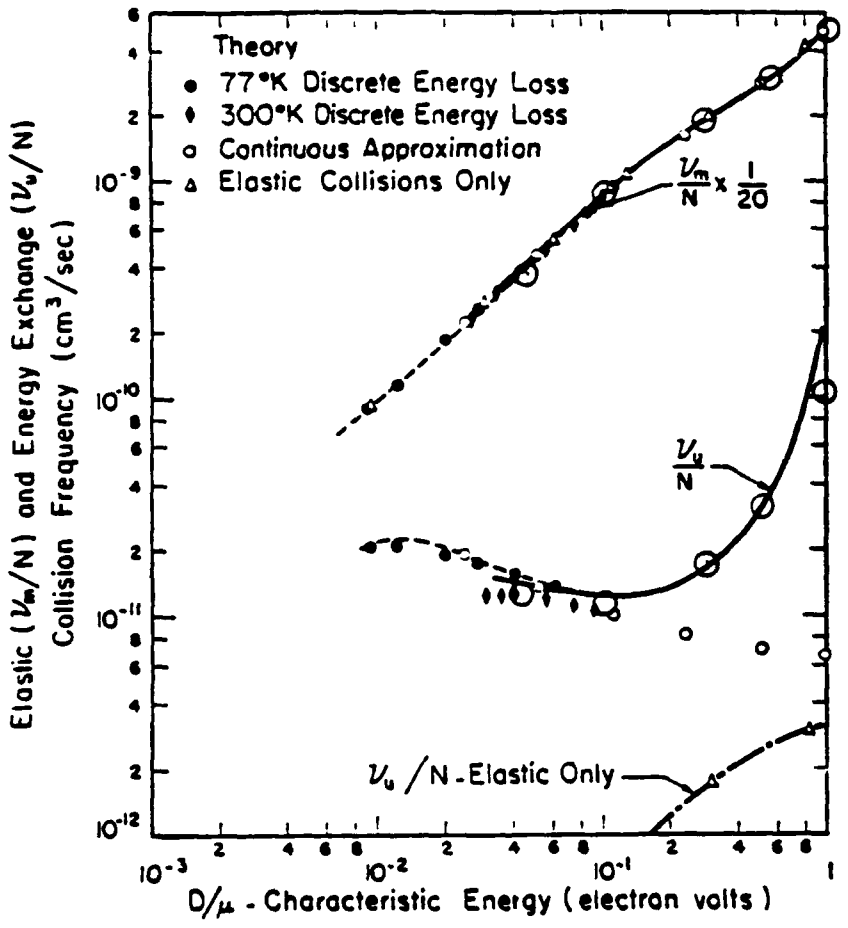

Figure 7. Swarm momentum transfer (ν_m/N) and energy transfer (ν_u/N) collision frequencies. The large open circles are our calculated values, superimposed on a graph from Frost and Phelps (Ref. 16). The solid curves are averaged experimental data at 300 K. The other four sets of points are various theories within Ref. 16.

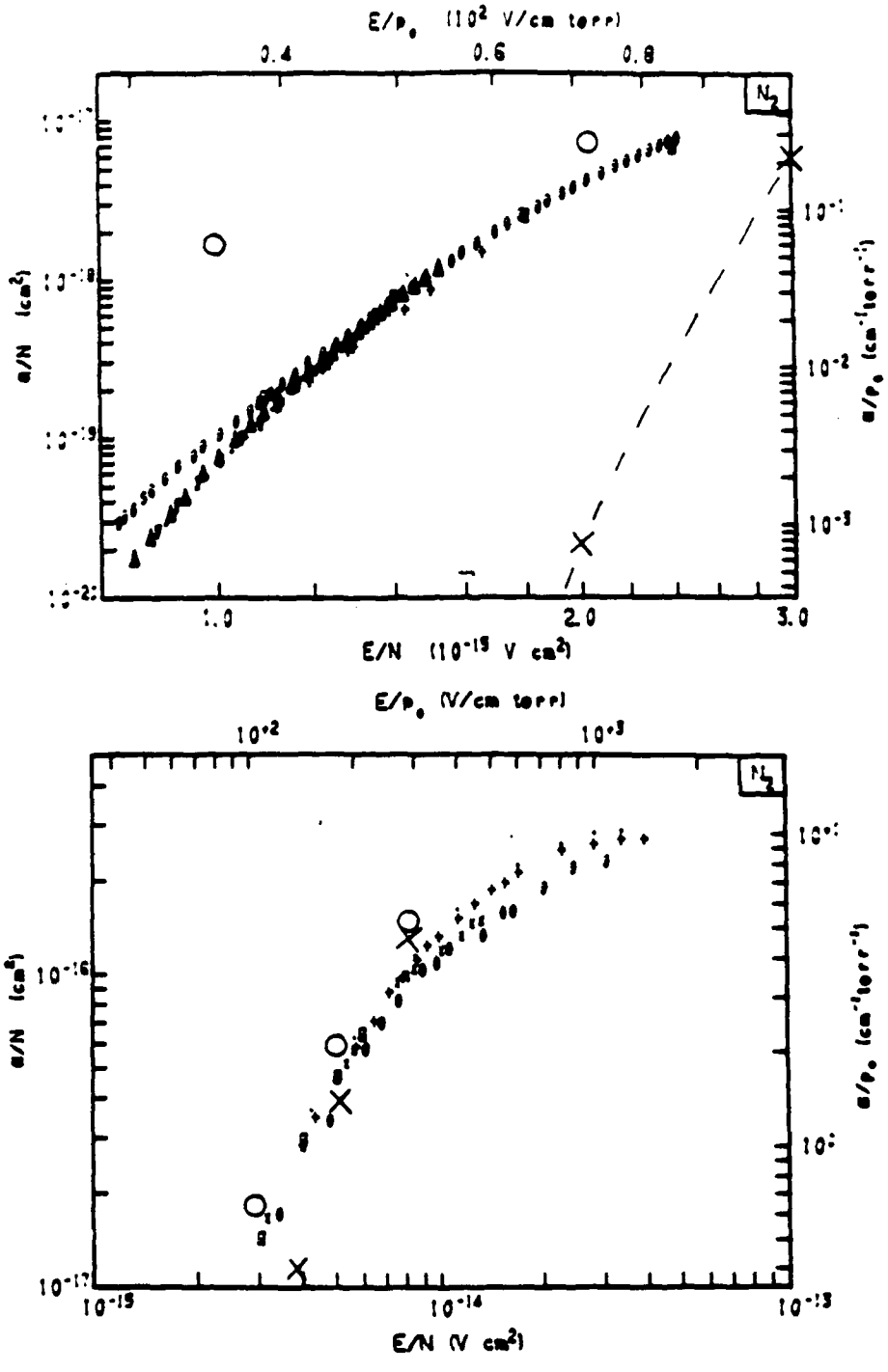

Figure 8. Calculated avalance rates (open circles) with data compiled by Dutton (Ref. 15). Crosses (x) are CSDA calculations.

2.16 STEADY STATE RESULTS FOR O_2

O_2 cross sections were collected in previous reports[2,4]. There is a discrepancy in the momentum-transfer cross section, it being more poorly understood in O_2 than N_2. We choose two alternate sets as in Reference 2. The first is the set recently recommended by Phelps[17], denoted in Figures 9 through 14 by open triangles; and the second is that of Wadzinski and Jasperse[18] corrected by Kieffer's[19] low energy tail, denoted by open circles.

The rotational cross sections are those of Gerjuoy-Stein with quadrupole moment Q = 1.8. For the vibrational cross sections, sharp spikes are smoothed out, choosing their energy integal to agree with Phelps' normalization.[17] The electronic cross sections are those compiled earlier by Archer[20] and in use by the DNA auroral physics community for years.

The resulting L and $\mathcal{M}$ are shown in Figure 9 at 300K. Rotational transitions are responsible for almost all energy loss below about 0.2 eV. The hump between 0.2 and 1 eV is due to vibrational transitions.

The spectrum F at $E/N_0 = 10$ and 100 Td is shown in Figure 10, along with that from the CSDA. Serious differences between the two are apparent at higher energies. Since many transport coefficients do not depend sensitively on the high energy tail the CSDA is not wildly different from either the L, $\mathcal{M}$ approximation or data, except for avalanching at low values of E/N_0.

Attachment has, of course, been ignored for the purpose of computing F, and we have found no published O_2 spectra computed with the full collision integral with which to compare the L, $\mathcal{M}$ approximation.

Figures 11, and 12 show the characteristic energy and drift velocity, drawn as circles and triangles over data compiled by Dutton. Below about 10^{-18}Vcm^2, differences in drift velocity between the two sets of momentum transfer cross sections, with each set agreeing with one set of data, reflect difficulties in performing drift velocity measurements in the electro-negative gas. Agreement is excellent over some five orders of magnitude in E/N_0.

Figure 13 is the momentum- and energy-transfer collision frequencies shown with more accurate calculations by Hake and Phelps[21]. With the momentum transfer cross section of Wadzinski and Jasperse[18,19] the agreement is striking, except in the energy-transfer frequency at 5 eV where electronic transitions cause a larger energy transfer rate than the Fokker-Planck expression predicts.

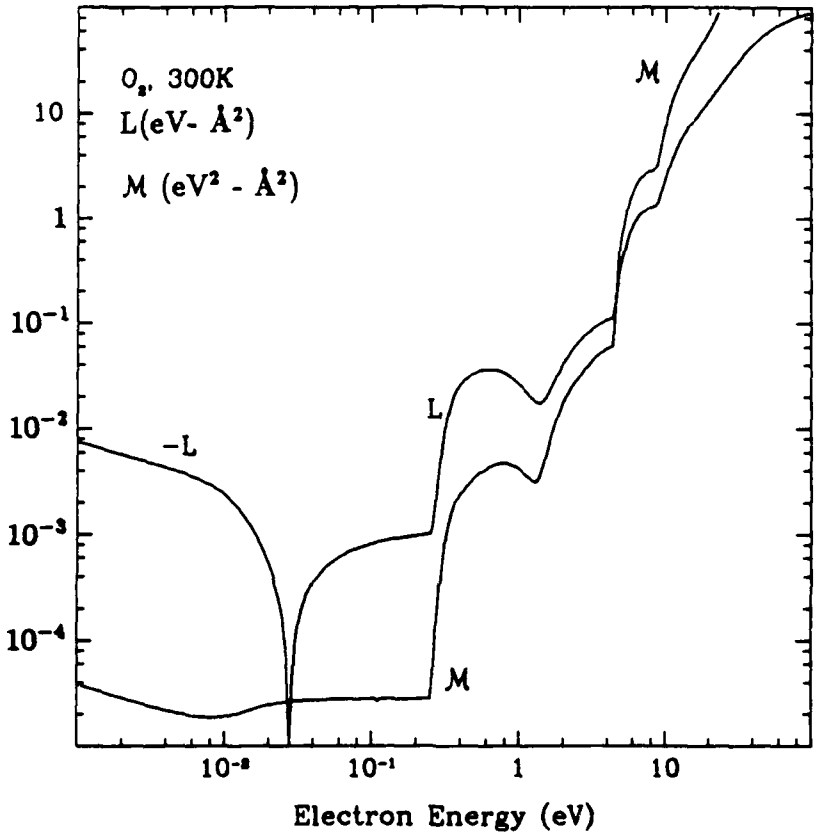

Figure 9. L and $\mathcal{M}$ for O_2 at 300 K. Quadropole moment = 1.8.

The avalanche rate in Figure 14 likewise confirms the excessive tail, as was the case in N_2.

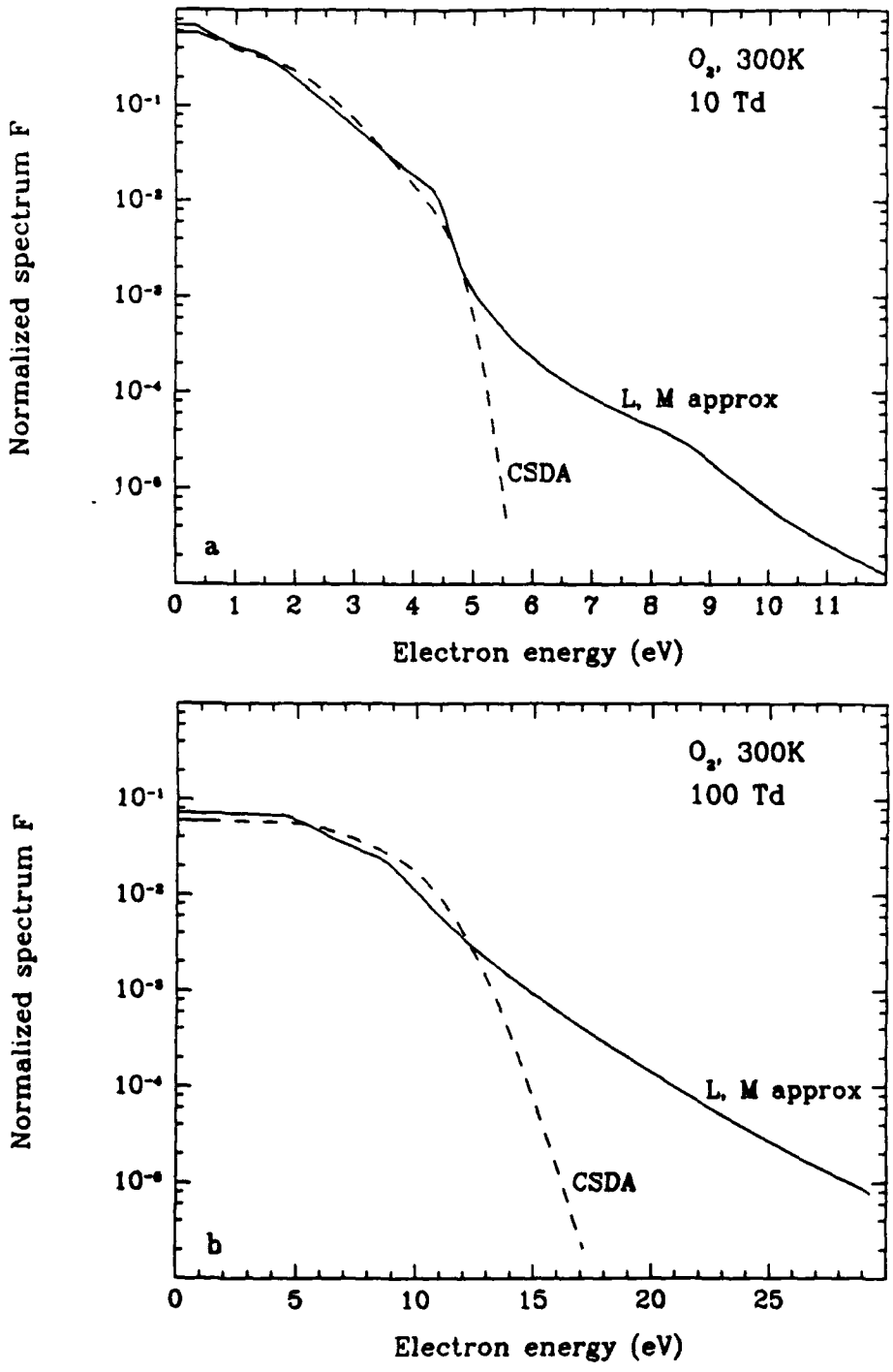

Figure 10. Energy spectrum in O_2 at $E/N_0 = 10$ and 100 Td.

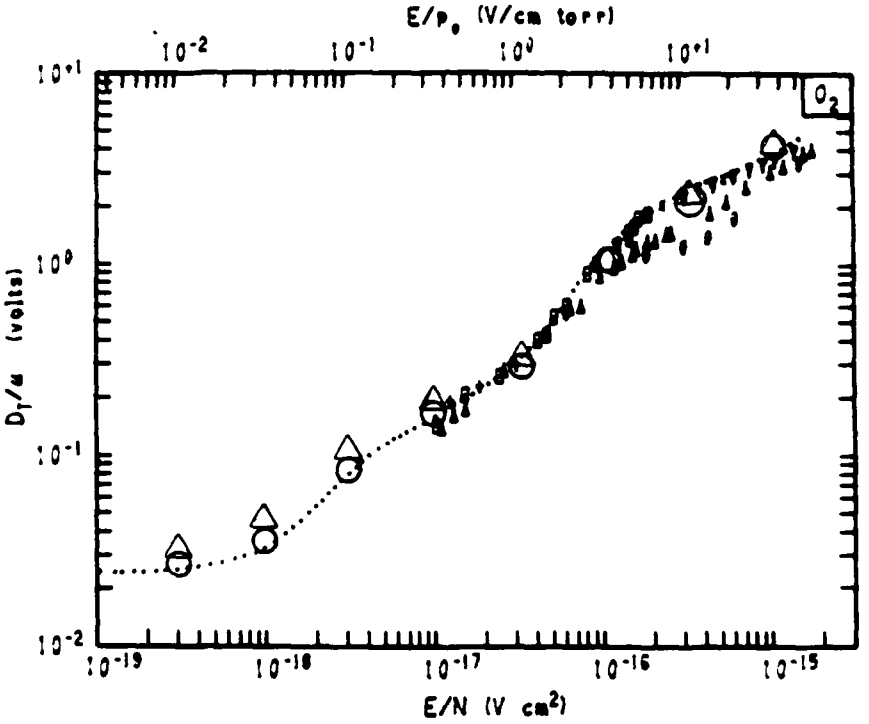

Figure 11. Characteristic energy vs E/N.

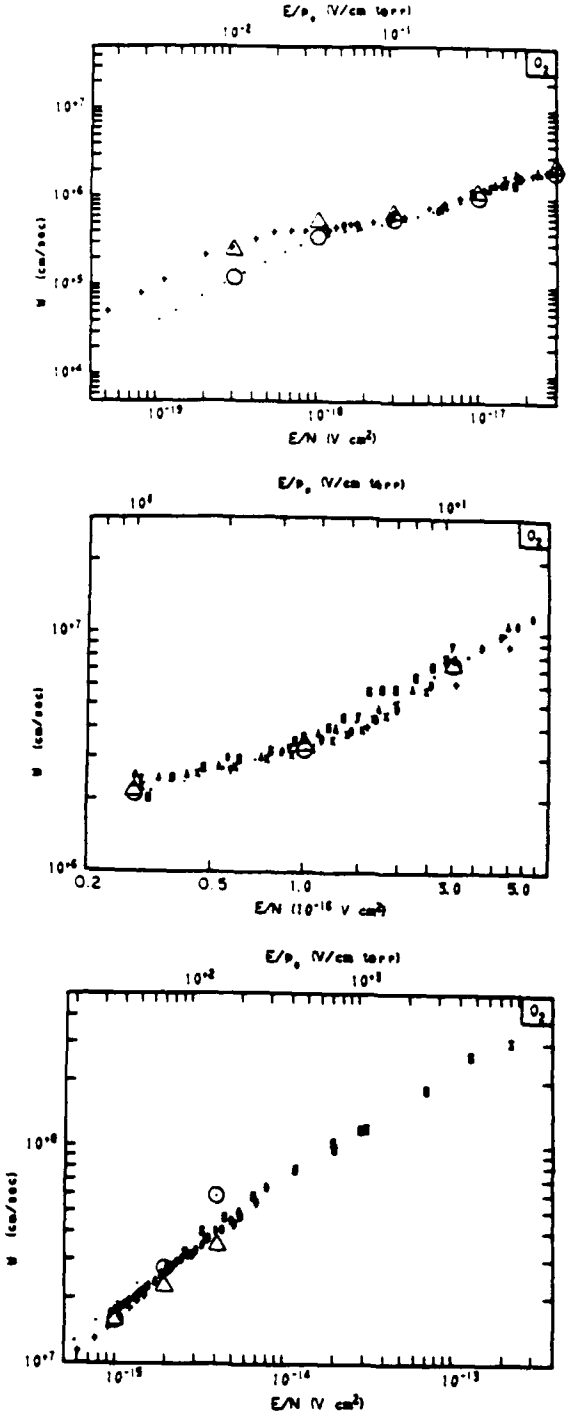

Figure 12. Drift velocity vs E/N.

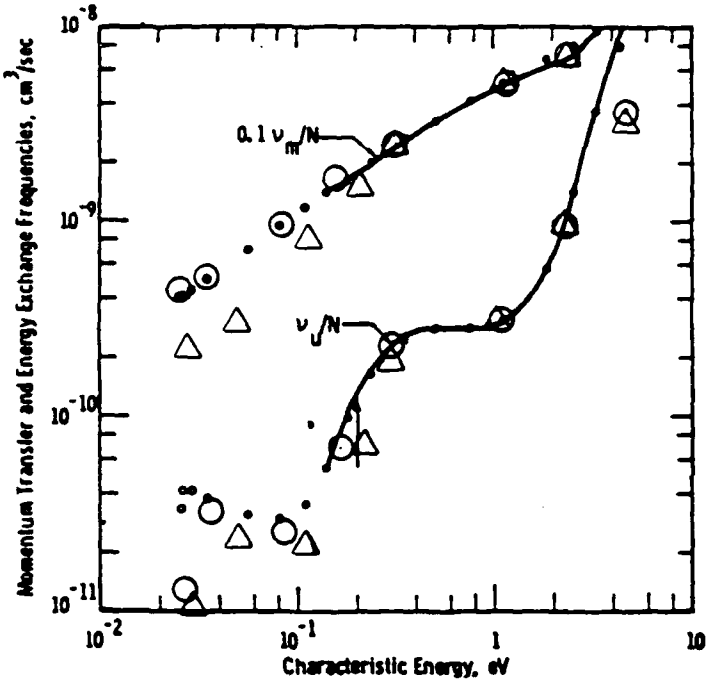

Figure 13. **Momentum-transfer and energy-exchange collision frequencies per molecule for electrons in oxygen.**

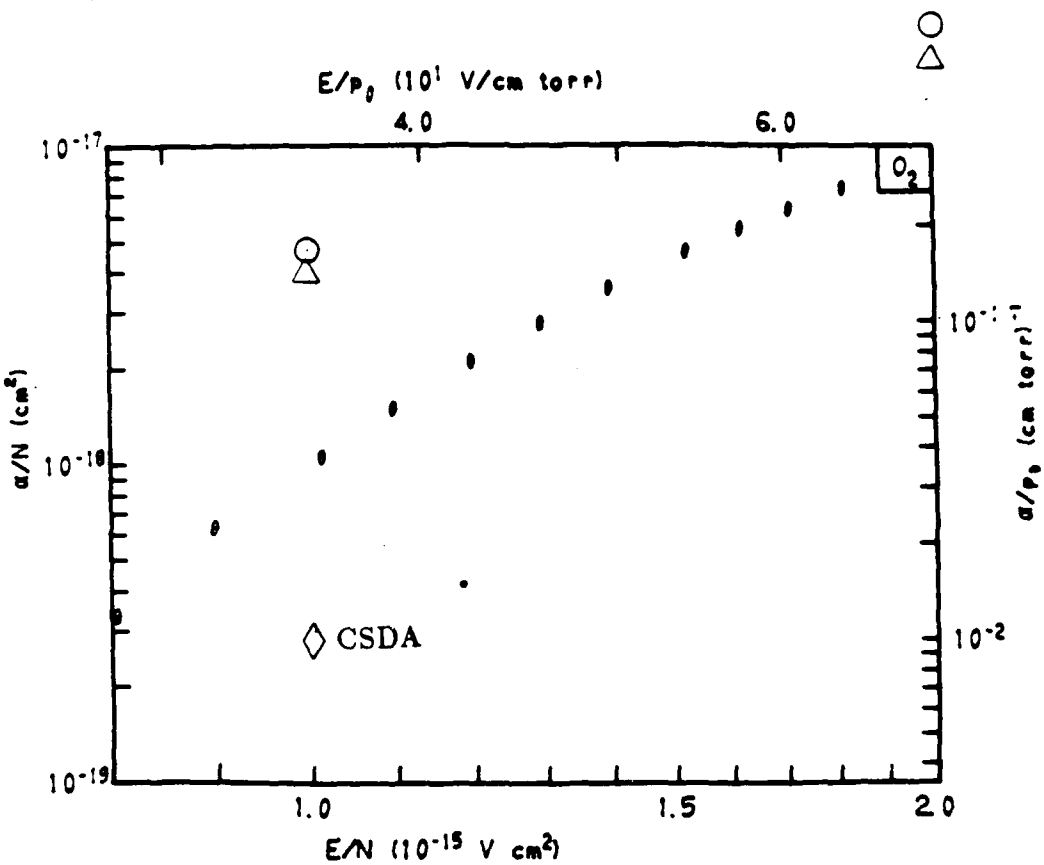

Figure 14. Avalanche rate.

SECTION 3

TIME DEPENDENT SPECTRA

Equation (31), together with sources or sinks on the right hand side, describes the time evolution of the distribution function F(w,t) in a constant or time varying electric field. It must be solved numerically. In this section we record the numerical integration scheme we have found most successful.

We need to solve

$$\frac{\partial F}{\partial \tau} = p\frac{\partial}{\partial w}\left(qF + r\frac{\partial F}{\partial w}\right) \quad , \tag{53}$$

where

$$\tau = N_0 t \tag{54}$$

$$p = v/w \tag{55}$$

$$q = w\left[L + \frac{1}{w}\frac{\partial}{\partial w}(w\mathcal{M})\right] \tag{56}$$

$$r = w\left[\frac{(eE/N_0)^2}{3\sigma_m} + \mathcal{M}\right] \quad , \tag{57}$$

with the initial condition $F(w,0) = F_0(w)$, over an energy range from w=0 to $w=w_{max}$. W_{max} depends on the problem, especially the sources, but it will be a few eV or more.

3.1 STABILITY CONDITIONS

Equation (53) has an advective term and a diffusion term. For explicit schemes a Courant stability condition

$$\Delta t < \frac{\Delta w}{pq} \quad , \tag{58}$$

and a diffusion stability condition

$$\Delta t < \frac{\Delta w^2}{2pr} \tag{59}$$

have to be met. An unconditionally stable implicit difference scheme would relax one or both stability criteria, but the accuracy condition is about the same; it would be dangerous to exceed these criteria by too much.

From 0 to w_{max} Figures 3 and 9 show q and r vary over several orders of magnitude. If one were to difference in w with constant energy spacing Δw, there would result an unacceptably small Courant time step at larger w with the large velocity pq and diffusion coefficient pr. Choosing increasing Δw would help solve this, but at the expense of lost centering in the spatial derivatives and therefore only first order accuracy.

3.2 CHOICE OF INDEPENDENT VARIABLE

Both problems can be alleviated by using the independent variable

$$u = \ell n(w + w_0) \quad , \tag{60}$$

where w_0 is a constant, so that Equation (53) becomes

$$\frac{\partial F}{\partial \tau} = P \frac{\partial}{\partial u} \left(QF + R \frac{\partial F}{\partial u} \right) \quad , \tag{61}$$

where

$$P = pu' \tag{62}$$

$$Q = q \tag{63}$$

$$R = ru' \tag{64}$$

$$u' = du/dw = \frac{1}{w + w_0} = e^{-u} \quad . \tag{65}$$

The stability criteria become

$$\Delta t < \frac{\Delta u}{PQ} = \frac{\Delta u}{pqu'} = \frac{(w + w_0)\Delta u}{pq} \tag{66}$$

and

$$\Delta t < \frac{\Delta u^2}{2PR} = \frac{\Delta u^2}{pru'^2} = \frac{(w + w_0)^2 \Delta u^2}{pr} \quad , \tag{67}$$

effectively making Δw proportional to w when one chooses constant Δu. w_0 is chosen larger than 0 so that $w = 0$ is a computation point. Differencing Equation (61) with constant Δu allows both spatial centering for second order accuracy and effectively increased cell size for larger time steps.

3.3 PHYSICAL TIME SCALES

The time scale for an electron to change its energy by δu is of order

$$T \sim \delta u/PQ \sim \delta w/pq \tag{68}$$

in the first term, and

$$T \sim \delta u^2/PR \sim \delta w^2/pr \tag{69}$$

in the second term. These time scales must be resolved for an accurate solution. But both of them are long compared to the time steps in Equations (66) and (67) if $\Delta u < \delta u$. Consequently, simply choosing Δu to resolve energy scales of interest guarantees a Δt that assures adequate resolution in the time evolution of F as well.

3.4 NORMALIZATION

Equation (53) preserves

$$\eta = \int_0^\infty \sqrt{w} F(w) dw \tag{70}$$

if there are no sources or sinks on the right hand side, and it is important that the difference algorithm does also. Experience with non-conservative difference schemes has shown that they do not preserve η accurately enough. We shall therefore choose a flux conservative differencing scheme.

3.5 DIFFERENCE SCHEME

Define energies w_i at points $i = 1,2,\cdots,N$ by

$$\begin{aligned} w_1 &= 0 \\ u_1 &= \ell n(w_1 + w_0) = \ell n(w_0) \\ u_i &= u_1 + (i-1)\Delta u \quad , \qquad i = 2,3,\cdots,N \\ w_i &= e^{u_i} - w_0 \end{aligned} \tag{71}$$

with $u_N = \ell n(w_{max} + w_0), \Delta u = (u_N - u_1)/(N-1)$. Define F at the same points,

$$F_i = F(u_i) \quad .$$

Integrating P^{-1} times Equation (61) between $u_i - \frac{1}{2}\Delta u = u_{i-1/2}$ to $u_i + \frac{1}{2}\Delta u = u_{i+1/2}$ gives the basic equation

$$\Delta y_i \frac{\partial F_i}{\partial \tau} = \left[QF + R\frac{\partial F}{\partial u} \right]\Bigg|_{i-1/2}^{i+1/2} \tag{72}$$

where

$$\Delta y_i = \int_{i-1/2}^{i+1/2} \frac{du}{P} = \int_{i-1/2}^{i+1/2} \frac{w}{v} dw \quad , \tag{73}$$

and we approximate the normalization element by

$$\int_{i-1/2}^{i+1/2} \frac{F}{P} du = \Delta y_i F_i \quad . \tag{74}$$

The form of Eq. (72) is flux conservative, preserving

$$\int \sqrt{w}\, F dw \propto \int \frac{w}{v} F dw = \sum_{i=2}^{N-1} \Delta y_i F_i + \text{boundary terms} \quad , \tag{75}$$

except for fluxes controlled by boundary conditions, since Eq. (72) says

$$\frac{\partial}{\partial \tau} \sum_{2}^{N-1} \Delta y_i F_i = \left[QF + R \frac{\partial F}{\partial u} \right]_{1+1/2}^{N-1/2} \quad . \tag{76}$$

The Crank-Nicholson implicit difference algorithm is used for Eq. (72). Setting

$$F_i^n = F(w_i, \tau_n) \quad , \tag{77}$$

Eq. (72) is advanced from τ_n to $\tau_{n+1} = \tau_n + \Delta\tau$ by

$$\frac{\partial F_i}{\partial \tau} = \frac{F_i^{n+1} - F_i^n}{\Delta \tau} \quad , \tag{78}$$

and the two terms on the right hand side at $i + 1/2$ are averaged at n and n+1,

$$(QF)_{i+1/2} = \frac{1}{2} Q_{i+1/2} \left\{ \frac{F_i^n + F_{i+1}^n}{2} + \frac{F_i^{n+1} + F_{i+1}^{n+1}}{2} \right\} \quad , \tag{79}$$

$$\left(R\frac{\partial F}{\partial u}\right)_{i+1/2} = \frac{1}{2}\left\{R^n_{i+1/2}\frac{F^n_{i+1}-F^n_i}{\Delta u} + R^{n+1}_{i+1/2}\frac{F^{n+1}_{i+1}-F^{n+1}_i}{\Delta u}\right\} \quad . \tag{80}$$

The right hand side at i - 1/2 is the same with i replaced by i - 1.

Boundary conditions are that the flux vanishes,

$$\left[QF + R\frac{\partial F}{\partial u}\right]\Bigg|_{1+1/2} = Q_{1+1/2}\frac{F^{n+1}_1 + F^{n+1}_2}{2} + R^{n+1}_{1+1/2}\frac{F^{n+1}_2 - F^{n+1}_1}{\Delta u} = 0 \tag{81}$$

$$\left[QF + R\frac{\partial F}{\partial u}\right]\Bigg|_{N-1/2} = Q_{N-1/2}\frac{F^{n+1}_{N-1} + F^{n+1}_N}{2} + R^{n+1}_{N-1/2}\frac{F^{n+1}_N - F^{n+1}_{N-1}}{\Delta u} = 0 \quad , \tag{82}$$

which guarantees normalization preservation.

The resulting implicit equations

$$\alpha_i F^{n+1}_{i+1} + \beta_i F^{n+1}_i + \gamma_i F^{n+1}_{i-1} = Z_i \quad , i = 1, 2, \cdots, N \tag{83}$$

require inverting only a tridiagonal matrix. The coefficients α_i, β_i, and γ_i are readily solved for in terms of the Q's and R's, and Z_i involves only quantities at time τ_n. Boundary conditions Eq. (81) and (82) are incorporated in Eq. (83). $\gamma_1 = \alpha_N = 0$.

The first nonzero computation energy is

$$\begin{aligned} w_2 &= e^{u_2} - w_0 = e^{u_1+\Delta u} - w_0 = w_0(e^{\Delta u} - 1) \\ &\approx w_0 \Delta u \end{aligned} \tag{84}$$

since $\Delta u \ll 1$. With N$\sim 10^2$, and w_{max} a few eV, Δu is typically $\Delta u \sim .05$. Then w_0 essentially controls w_2. Desiring $w_2 \sim 10^{-3}$ eV means w_0 should be chosen of order .02.

For the first few cells $i\Delta u \ll 1$, and w_i is equally spaced with spacing $\Delta w \sim w_2$. Then the energy spacing starts to increase, with

$$\Delta w_i = w_{i+1} - w_i = e^{u_i+\Delta u} - e^{u_i} = e^{u_i}(e^{\Delta u} - 1) = (w_i + w_0)(e^{\Delta u} - 1) \approx (w_i + w_0)\Delta u \quad (85)$$

approximately linearly increasing with w when $w_i > w_0$.

We now investigate time dependent spectra with and without an electric field using numerical solutions of Eq. (31).

SECTION 4

RELAXATION OF THE SPECTRUM IN THE ABSENCE OF FIELDS

In the absence of an electric field, collisions cause an initial distribution to relax toward thermal equilibrium in the host gas, a process described in the L, $\mathcal{M}$ approximation by Equation (29), or Equation (31) with E = 0. The spectrum starts at F(w,t=0) = F_0(w). We can study in particular the difference in the evolving spectra between the CSDA and when the correct $\mathcal{M}$ is used.

We use the numerical solution of Equation (53) described in Section 3. With E = 0 the formulation is not restricted to the first two Legendre terms, and so applies to electrons of any energy, so long as their fractional energy loss per collision remains small. Nevertheless we are mostly concerned with electrons of relatively small energies, the so-called swarm regime. Only the motion of primary electrons is treated; increasing numbers by avalanching is not included.

4.1 RELAXATION IN O_2

Consider a hot electron swarm in room temperature O_2. We arbitrarily choose F_0(w) to be a Maxwellian at T_e = 0.2 eV, and follow the evolution of the spectrum toward a Maxwellian at 300K = 0.026 eV, ignoring attachment.

Figure 15 shows the spectrum at six times, starting at t = 0. It begins to pile up near 0.2 eV because only relatively slow rotational transitions can reduce it from there. The bunching follows the small values of L seen in Figure 9. It has essentially reached its final Maxwellian value by $N_0 t = 2 \times 10^{11} s/cm^3$.

At the final time, between about 0.01 eV and 0.25 eV, the calculated distribution is exp(-w/T_e), with T_e = .026 eV, as it must be. At smaller energies it departs from Maxwellian because rotational transitions are comparable to w, as discussed in Section 2.9. At higher energies it is smaller than Maxwellian because we have not included thermally populated vibrational levels in the gas.

Figure 16 shows the same times for the CSDA. Comparing with Figure 15 the effect of $\mathcal{M}$ in elevating the tail, and in spreading out the peaks, is obvious.

A blow up of the low energy region is shown in Figure 17 for both the CSDA

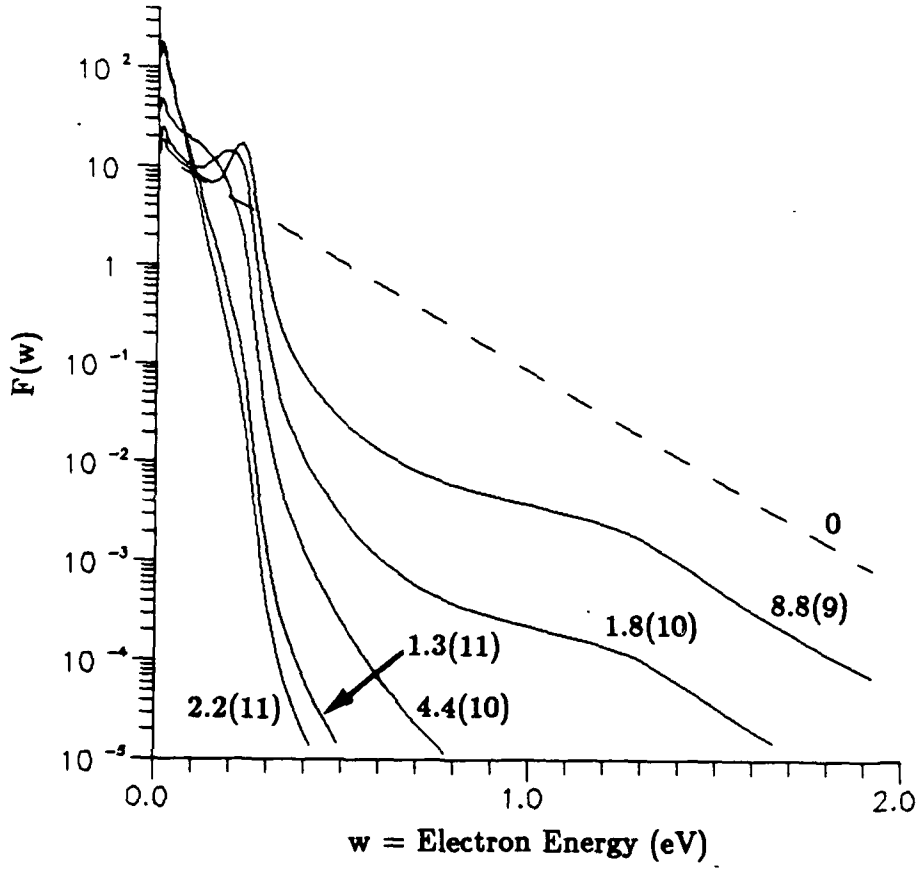

Figure 15. Relaxation of the energy spectrum in O_2 in the L, M approximation. 4.4(10) means $4.4\times10^{10}s/cm^3$, etc..

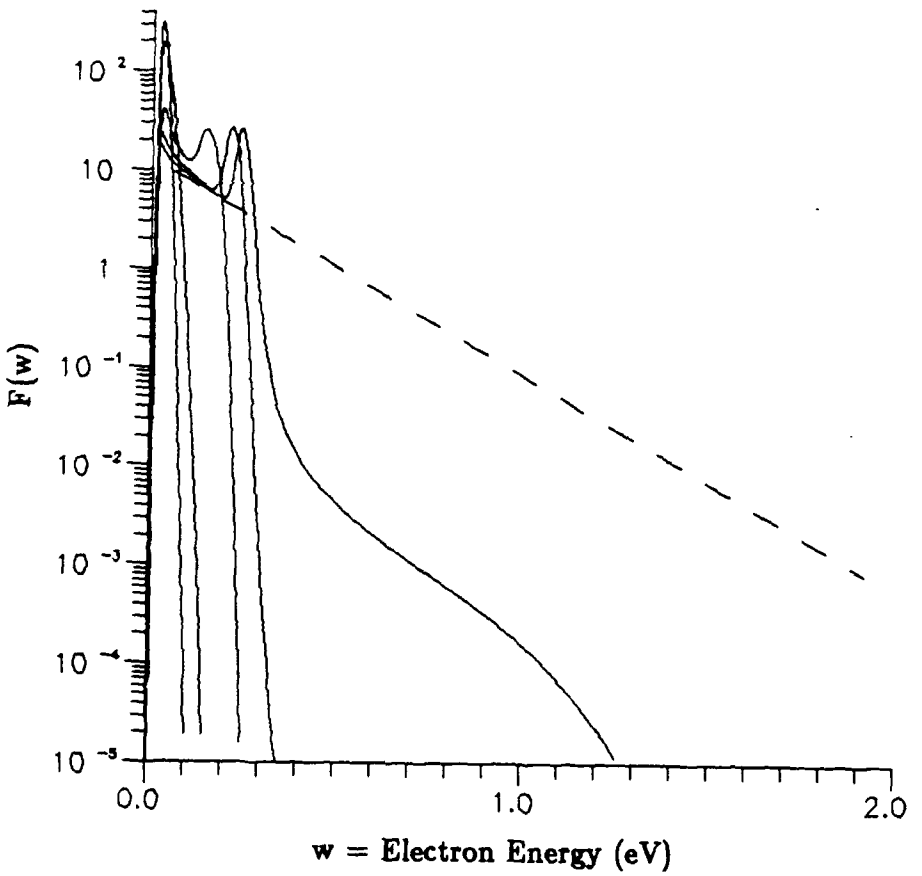

Figure 16. Relaxation of the energy spectrum in O_2 in the CSDA. Same successive times as Figure 15.

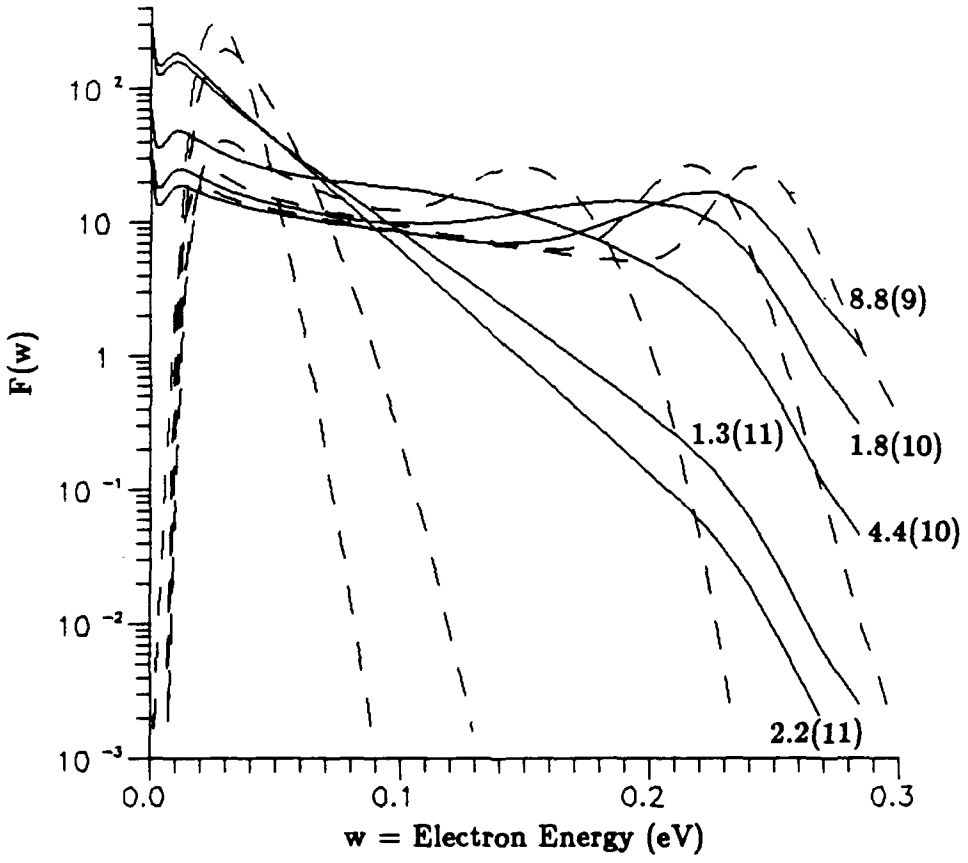

Figure 17. Low energy detail of relaxation in O_2 in the L, M approximation (solid) and in the CSDA (dashed).

(dashed lines) and when the correct $\mathcal{M}$ is employed.

The CSDA spectrum has not quite collapsed to a delta function at the last time because a small diffusion coefficient was retained for code stability.

The decay of the instantaneous characteristic energy $\epsilon = D_T/\mu$ where D_T is the transverse diffusion coefficient and μ the mobility, and the average energy $\bar{w}$, are shown in Figures 18a and b. $\bar{w}$ differs only slightly whether $\mathcal{M}$ is retained or not, in accordance with the discussion following Equation (34). ϵ is seen to differ considerably more.

The growth of the swarm mobility in the two cases is shown in Figure 19. A gas density of $N_0 = 3.36 \times 10^{16} cm^{-3}$ has been assumed to obtain mobility in m/s/V/m. In the CSDA the mobility always lags behind the correct value. This result, together with a similar one for air discussed below, suggests that mobility or conductivity calculations in actual cases may likewise be inaccurate by comparable amounts if the CSDA were used.

4.2 RELAXATION IN AIR

Figure 20 shows the Loss Function L for air ($.79N_2 + .21O_2$). Spectrum relaxation in the L, $\mathcal{M}$ approximation is shown in Figure 21 with the complete $\mathcal{M}$, and in Figure 22 in the CSDA. Differences between them are similar to the case of O_2. In the CSDA the distribution above 1.5 eV is completely gone after only $N_0 t = 8 \times 10^9 sec/cm^3$, and is gone above 0.5 eV after only $4 \times 10^{10} sec/cm^3$. The broad hump in the distributions in Figure 21 near 4 eV is electrons lingering in the hollow in L between the resonance peak and the onset of electronic transitions.

Figures 23a and b show the decay of the characteristic energy and the average energy, while Figure 24 depicts the growth of the mobility. Even though the L, $\mathcal{M}$ approximation results in a distribution with a higher tail, the characteristic energy is dominated by low energy electrons and is higher in the CSDA (by almost a factor of two at $2 \times 10^{11} s/cm^3$), causing mobility to be lower in the CSDA.

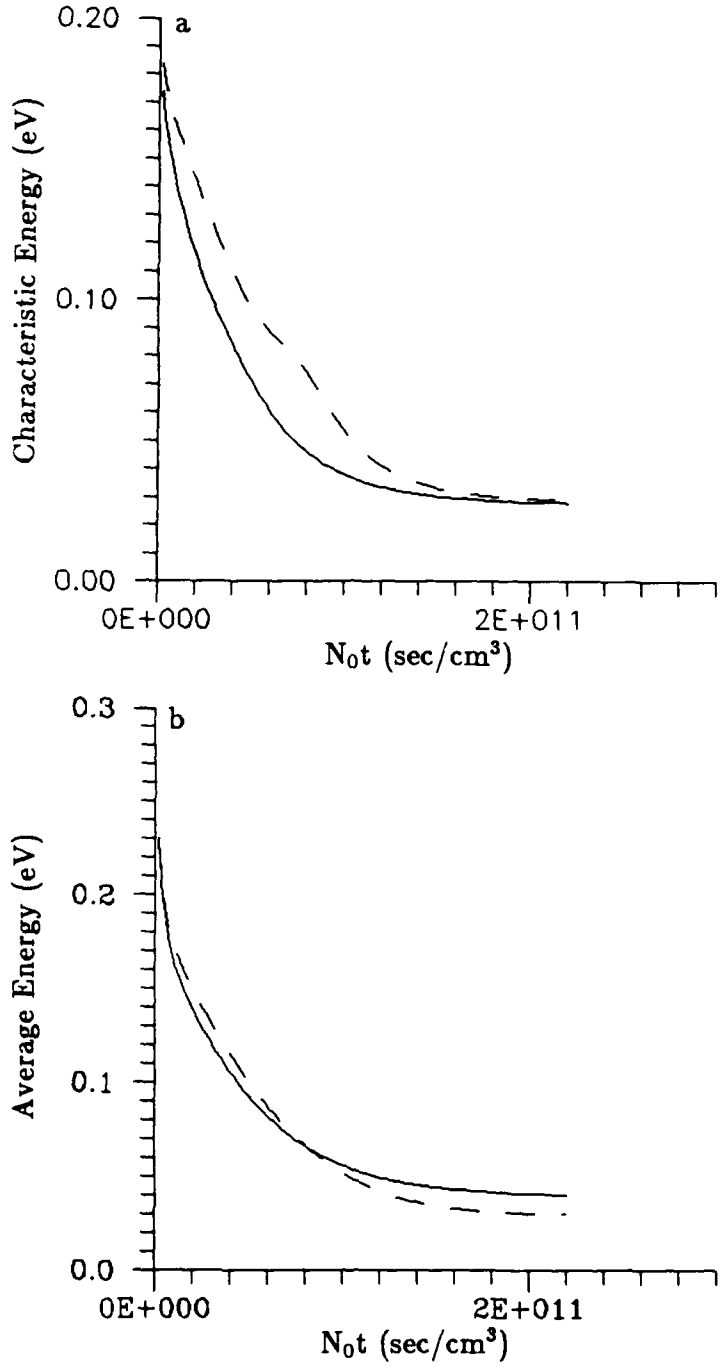

Figure 18. **Evolution of the characteristic energy (a) and average energy (b) in O_2 in the L, M approximation (solid) and CSDA (dashed).**

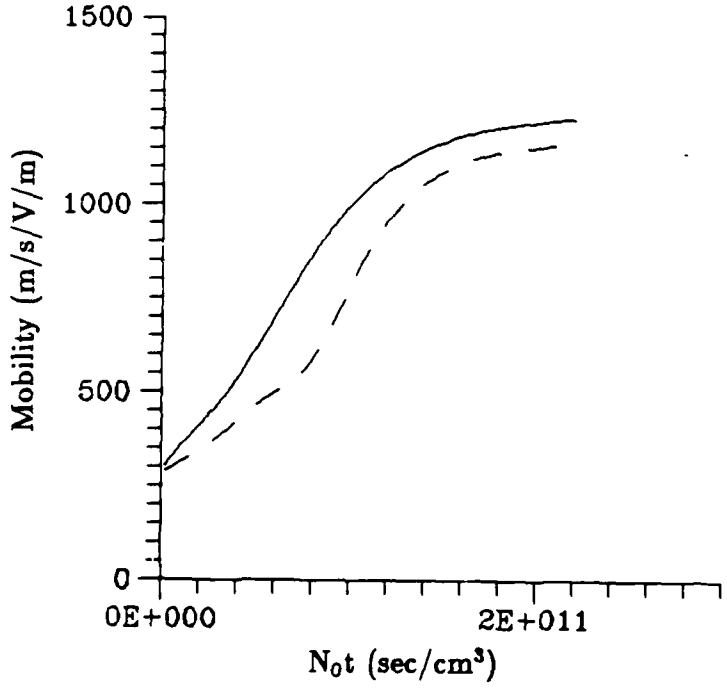

Figure 19. Evolution of the mobility in O_2. L, M approximation (solid); CSDA (dashed).

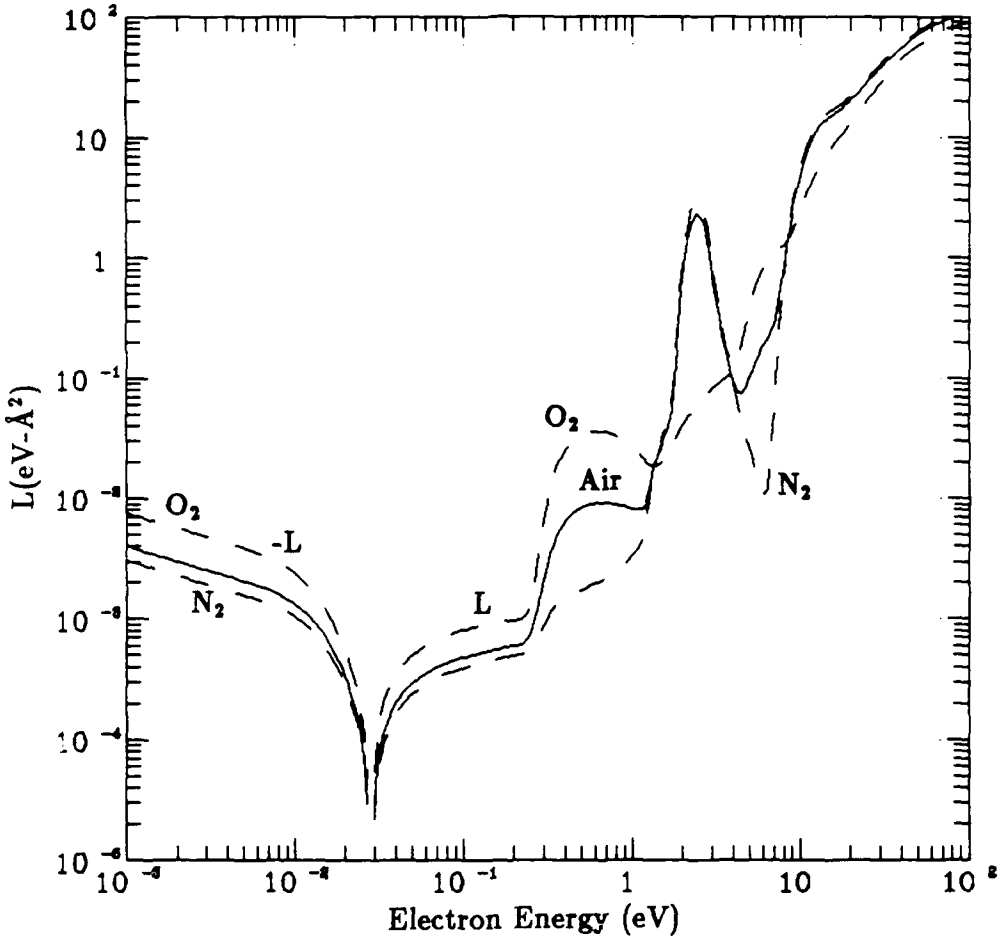

Figure 20. Loss function in O_2, N_2 (dashed), and air (solid).

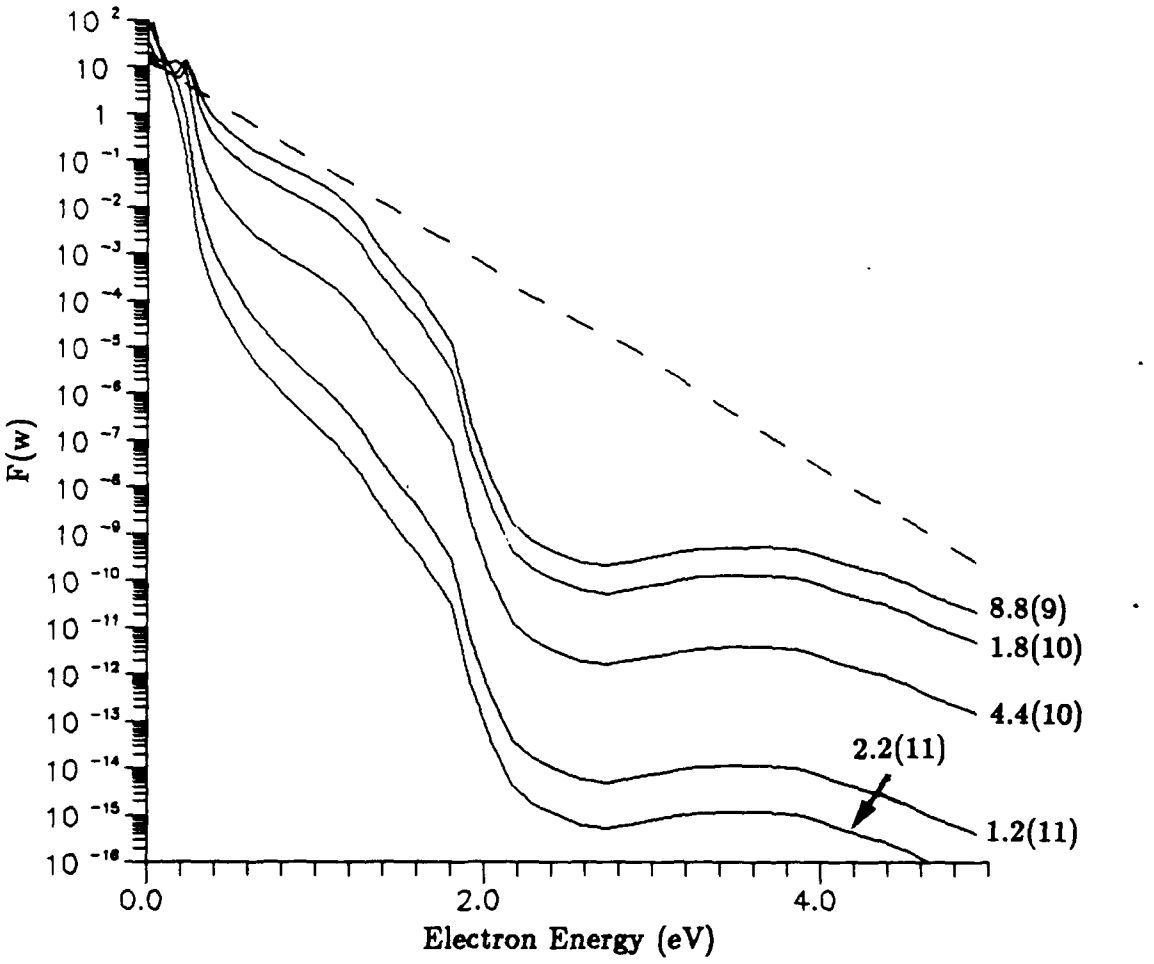

Figure 21. Relaxation of the energy spectrum in air in the L, M approximation.

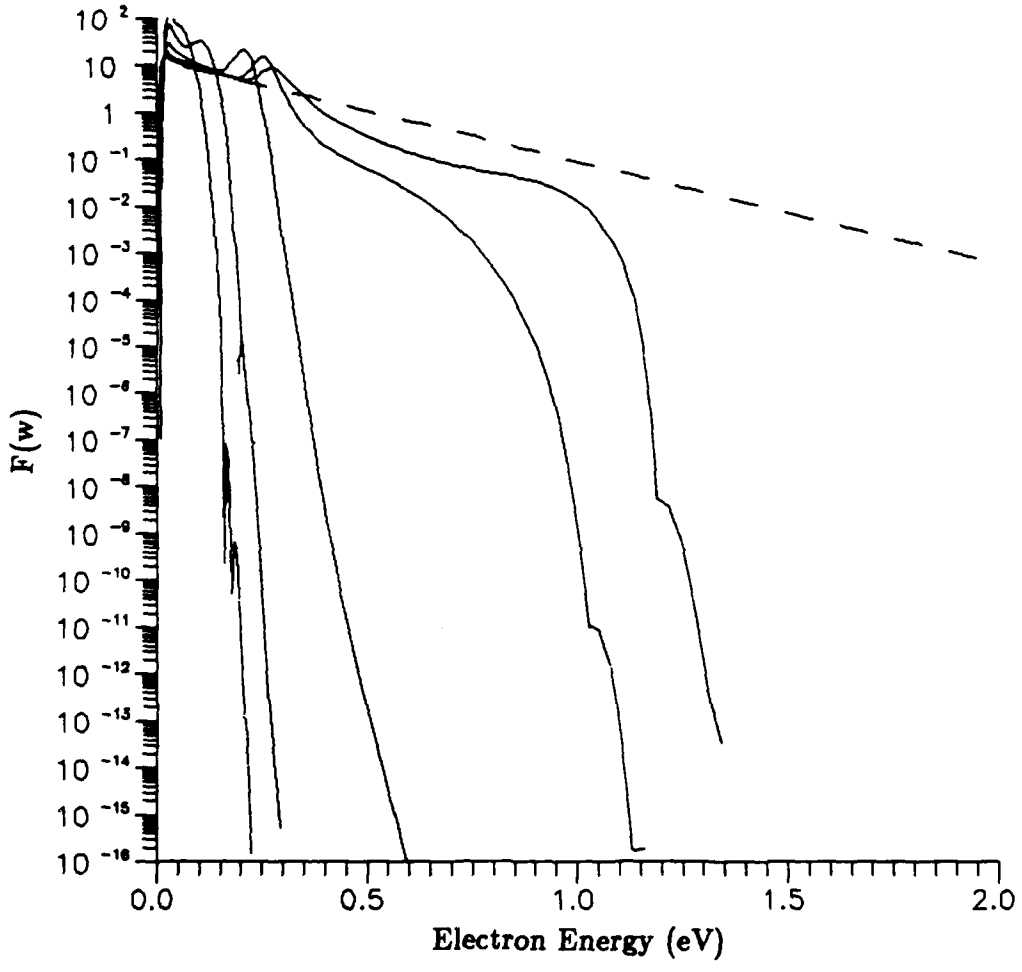

Figure 22. Relaxation of the energy spectrum in air in the CSDA. Same successive times as in Figure 21.

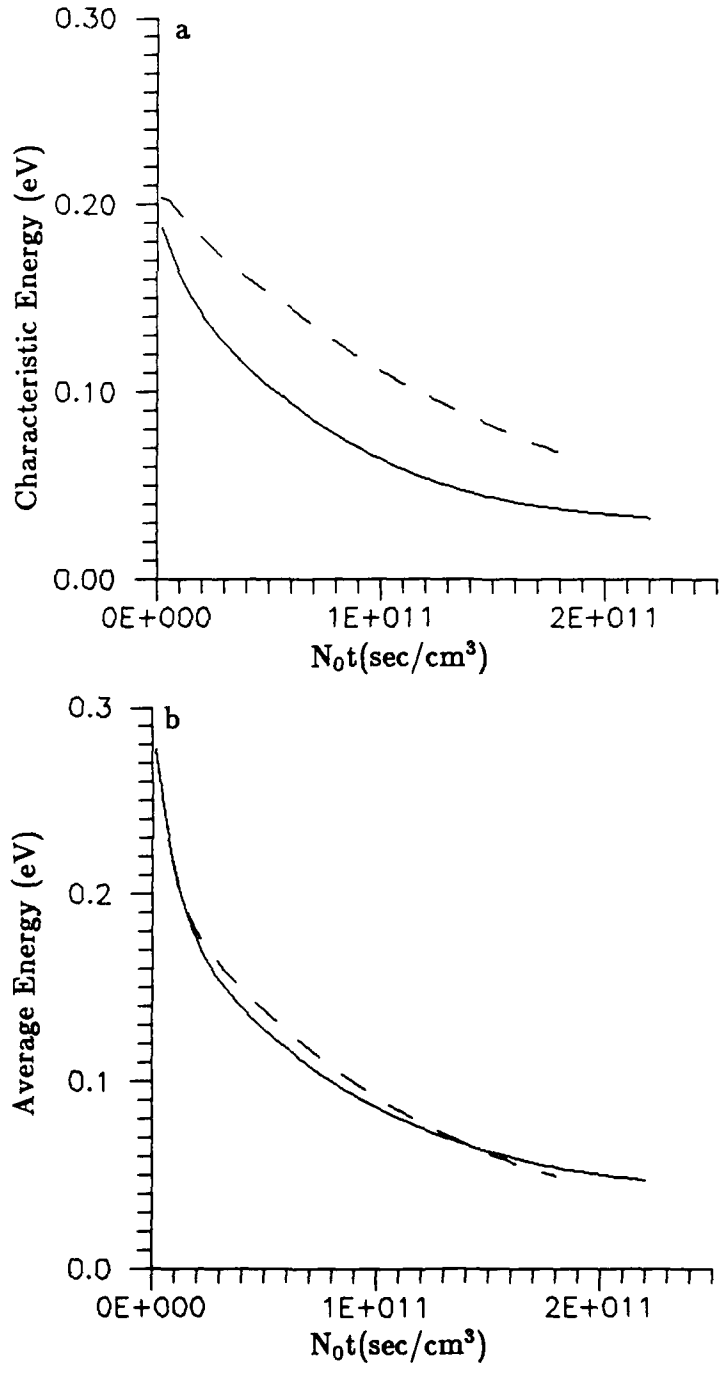

Figure 23. Evolution of the characteristic energy (a) and average energy (b) in air in the L, M approximation (solid) and CSDA (dashed).

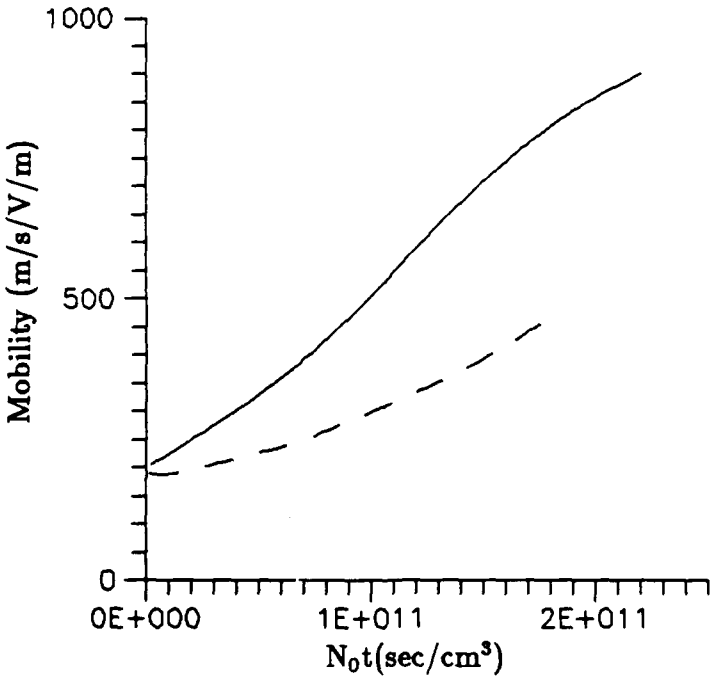

Figure 24. Evolution of the mobility in air. L, M approximation (solid); CSDA (dashed).

SECTION 5

SPECTRAL BEHAVIOR FOLLOWING A TIME VARYING ELECTRIC FIELD

Except for spectral lag effects which require a time of order $1/\nu_u$, the time scale for the drift velocity of a swarm to readjust in a varying electric field is $1/\nu_m$, arising from the randomizing of directed velocities due to momentum transfer scatterings. The time scale for the energy spectrum to equilibrate in a changing field is $1/\nu_u$, the inverse of the swarm energy transfer collision frequency. These frequencies were shown as a function of swarm characteristic energy in Figures 7 and 13 for N_2 and O_2, respectively.

Generally $\nu_m >> \nu_u$. Thus there is an interesting time region in which electric fields vary slowly compared with ν_m but not slowly compared with ν_u. The L, $\mathcal{M}$ approximation is valid in just this regime, and can exhibit time lag effects in relatively rapidly varying fields.

As an example, the EMP from high altitude nuclear detonations is produced by γ rays depositing at altitudes between about 20 and 40 km creating Compton electrons which then produce secondary ionization. The secondary electrons are a swarm, which drifts in the self-consistent electric field making a conduction current. At 30 km, for example, $N_0 = 3.8\times10^{17}cm^{-3}$, and $1/\nu_u \approx 1.3\times10^{-8}$ sec for characteristic energy $\epsilon = 1$ eV. This time is comparable to the time scale of the changing electric field, and so the swarm energy spectrum lags the field in equilibrating to its new value. Thus the swarm mobility would not be given correctly by its steady state value in the instantaneous field.

To demonstrate spectral time lag effects we calculate here the time dependent spectrum and transport coefficients of an originally thermal swarm in a rapidly varying pulsed electric field. We do so in air in spite of the fact that it stresses the Fokker-Planck approximation, as mentioned in the discussion of N_2. The field is turned on at $t = 0$ and then taken to vary as a sine wave for half a period:

$$\begin{aligned} E &= E_0 \sin(\pi t/T_0), \qquad t < To \\ &= 0, \qquad\qquad\quad t > T_0 \end{aligned} \tag{86}$$

An air density of $3.83 \times 10^{17} cm^{-3}$ is chosen to correspond to an altitude of 30 km. We choose a peak field of $E_0 = 3.83 \times 10^3$ V/m, corresponding to $E_0/N = 10$ Td. In the peak field in steady state this would give the swarm a characteristic energy of $\epsilon = 1$ eV. Thus a useful time scale is $1/\nu_u$ (1 eV). From Figures 7 and 13, at the chosen density, this time is $\approx$ 12 ns.

Since the swarm starts at thermal energies, the calculation is not meant to apply to high altitude nuclear EMP, but is intended to illustrate time lag effects, and the usefulness of the L, $\mathcal{M}$ approximation in quickly calculating spectral behavior.

5.1 RAPIDLY VARYING FIELD

We first choose $T_0 = 2.5 \times 10^{-8}$ sec, so the field peaks in about $1/\nu_u$ (1 eV). However, this time variation is rapid enough that the characteristic energy, which starts at 0.026 eV, never rises to 1 eV before the pulse is over, since ν_u is much less for lower energies.

The field, characteristic energy, and mobility are shown in Figure 25. ϵ rises to only about 0.13 eV at 20 ns. The lower dot-dashed curve shows what the energy ϵ_{inst} would be if the spectrum equilibrated immediately to the instantaneous field. When the pulse terminates, $\epsilon \approx 0.12$ eV. At this energy, $1/\nu_u \approx 150$ ns, and the spectrum and ϵ subsequently relax very slowly, lingering for a long time at almost four times its final value.

The mobility μ in very weak fields is about 100 (m^2/Vs). It likewise never reaches its steady state value in the peak field, achieving a minimum of only about 25 (m^2/Vs). The upper dot-dashed curve shows what the mobility μ_{inst} would be if the spectrum equilibrated instantaneously. For both the mobility and characteristic energy there is almost an order of magnitude discrepancy during most of the pulse.

5.2 MORE SLOWLY VARYING FIELD

As another example, we slow the field down by a factor of 4, choosing $T_0 = 1 \times 10^{-7}$ sec. This will allow transport coefficients to more nearly approach their steady state values.

Figure 26 shows the same quantities. The characteristic energy in this case reaches 0.65 eV at 75 ns and then decays at a varying rate; ν_u decreases as ϵ decreases.

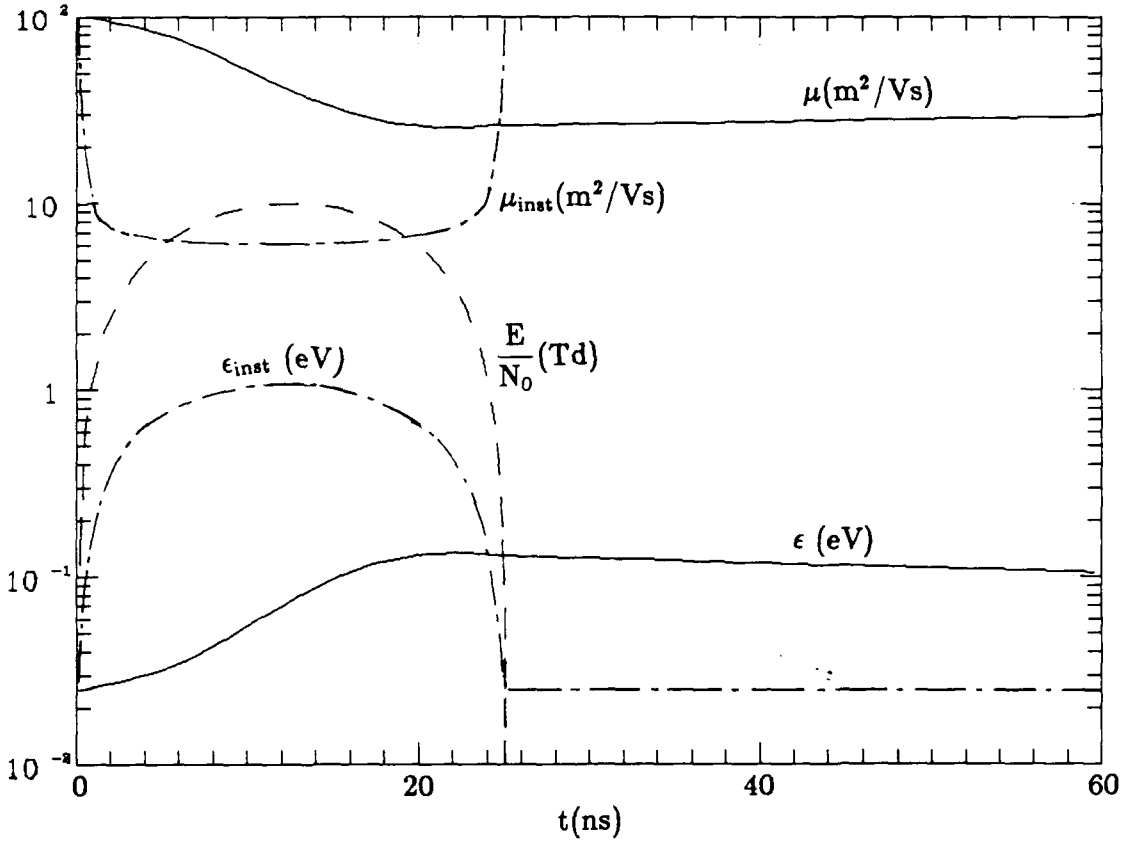

Figure 25. Characteristic energy ϵ and mobility μ in a pulsed electric field in air lasting 25 μs.

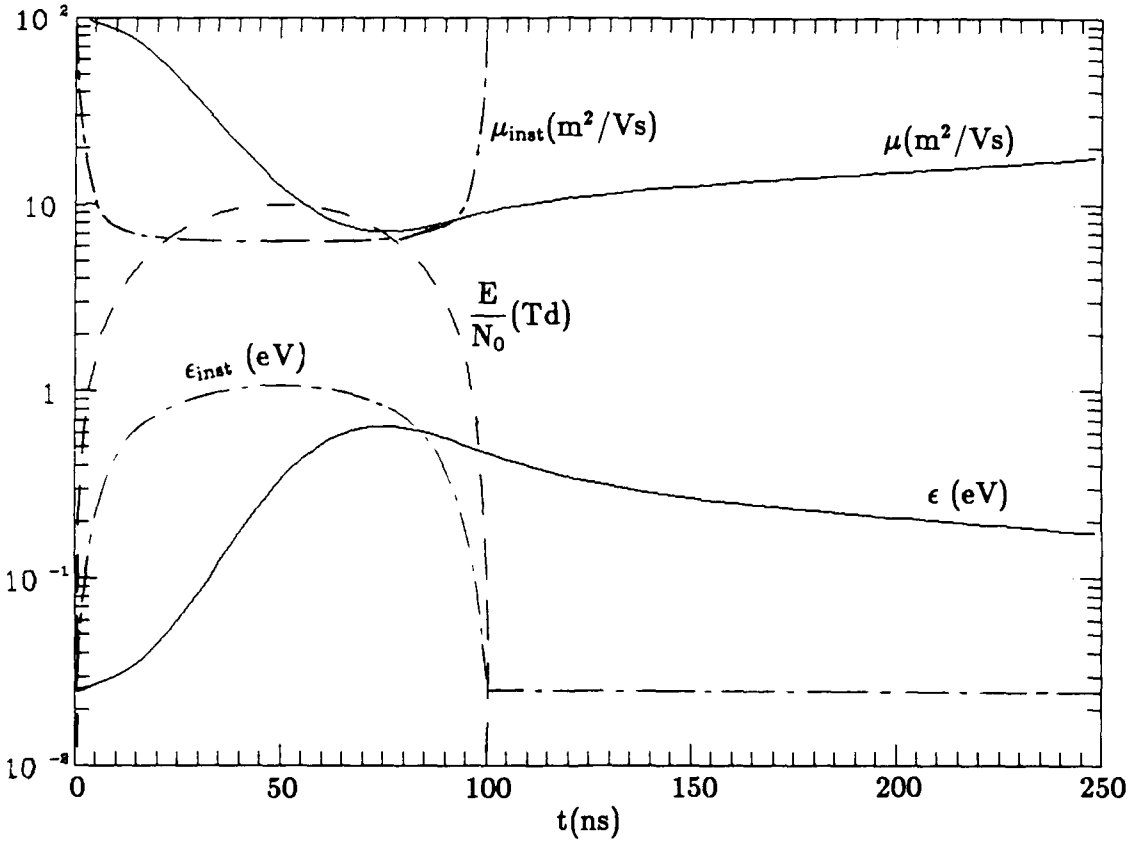

Figure 26. Characteristic energy ϵ and mobility μ in a pulsed electric field in air lasting 100 ns.

The mobility almost achieves its steady state value (6 m^2/Vs) in the peak field before the pulse is over. Both ϵ and μ exhibit a time lag of about 50 ns relative to the field, being an average of $1/\nu_u$ in the swarm as it heats.

Figure 27 shows the energy spectrum for this case at 20, 40, 60, 100, and 200 ns, starting at a 300K Maxwellian at t = 0 (dashed line). At each time the spectrum is far from its equilibrium value in the instantaneous field (not shown).

5.3 FINAL COMMENT

The L, $\mathcal{M}$ approximation reduces the integro-differential Boltzmann Equation to a differential equation, which may be solved by standard finite difference numerical methods. The equation contains most of the physics determining the spectrum, and is accurate when the fractional energy loss per energy-transfer collision is small. It is more accurate than the CSDA, is conceptually more complete, and does not violate detailed balance.

Here we have explored only the cases of spectrum relaxation in the absence of fields, and spectral lag in rapidly varying fields. One could easily include prescribed sources and chemistry on the right hand side to treat more general problems. References 1 and 2 presented a more detailed treatment of the theory, and a more thorough discussion of the steady state spectra and transport coefficients in N_2 and O_2.

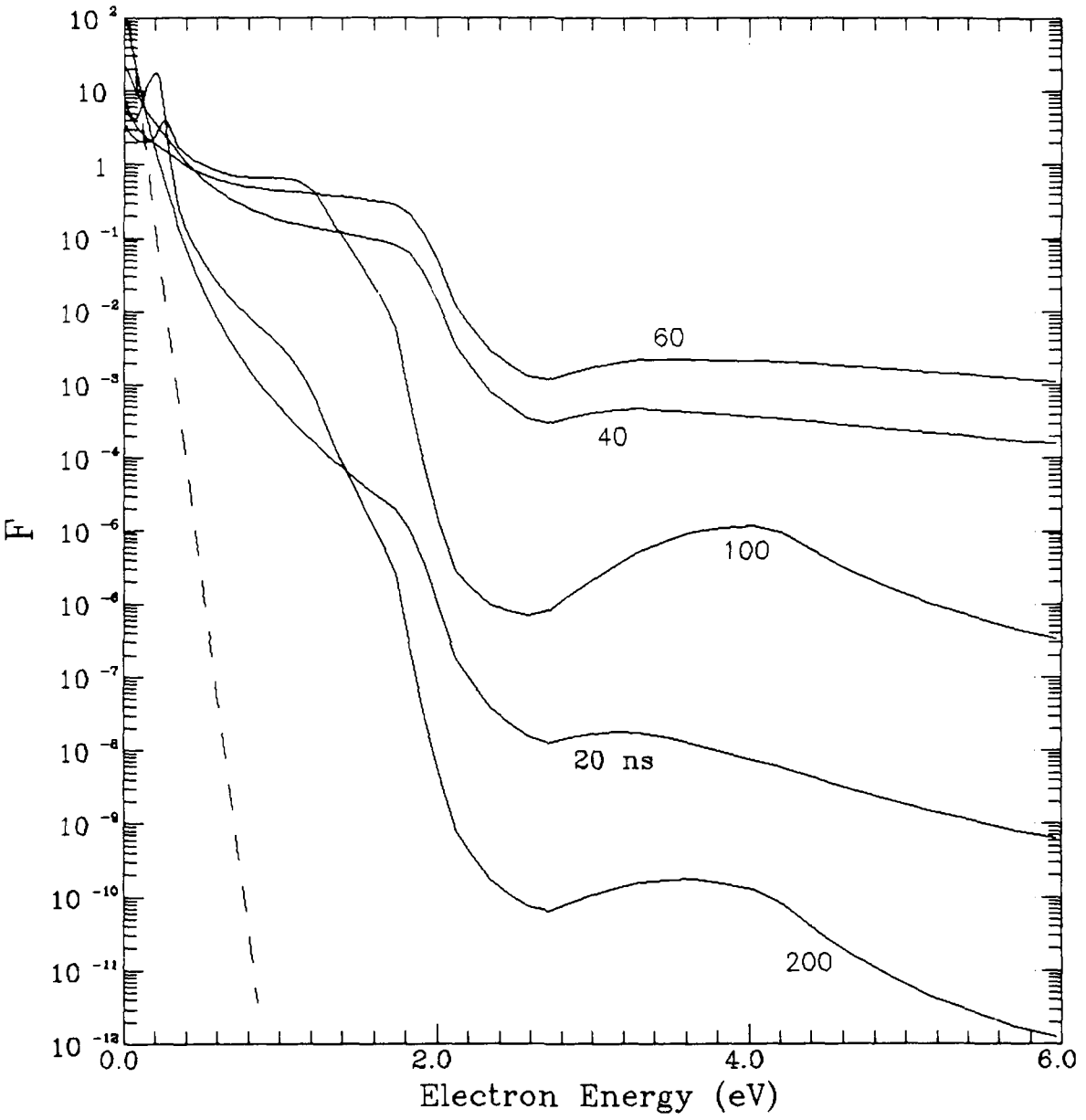

Figure 27. Electron energy distribution function at t = 0 (dashed) and five later times (solid) for 100 ns pulse length.

REFERENCES

1. Carron, N. J., "On the Calculation of the Electron Energy Spectrum in a Weakly Ionized Gas", MRC-R-1055 Revised, 30 January 1987

2. Carron, N. J., "Advances in the Approximate Electron Energy Spectrum Theory and Application to O_2", MRC-R-1135, 28 January, 1988

3. Goldstein, B. M., "A Summary of Rotational and Vibrational Cross Sections in N_2", MRC-R-1057, 26 January 1987.

4. Goldstein, B. M., "Electronic Excitation of the Vibrational and Rotational States of Molecular Oxygen", MRC-N-819, June 15, 1988.

5. The equilibrium Maxwell distributions for a gas of temperature T, which obtain when $E = 0$, are $f_M = n(m/2\pi T)^{3/2}\exp(-mv^2/2T), F_M = 4\pi f_M, g_M = (2/\sqrt{\pi})(n/T)\sqrt{w/T}\exp(-w/T)$.

6. Shkarofsky, I. P., T. W. Johnston, and M. P. Bachynski, *The Particle Kinetics of Plasmas*, Addison-Wesley, 1966.

7. Allis, W. P., "Motions of Ions and Electrons", in *Handbuch der Physik*, Springer-Verlag, Berlin, 1956, Vol. XXI.

8. Huxley, L. G. H., and R. W. Crompton, *The Diffusion and Drift of Electrons in Gases*, J. Wiley 1974. Section 6.9.

9. Pidduck, F. B., Proc. Roy. Soc. A, 88, 296 (1913); Proc. Lond. Math. Soc., 15, 89 (1916); Quart. J. Math., 7, 199 (1936)

10. Davydov, P., Phys. Z. Sowjetunion, 8, 59 (1935)

11. Morse, P. M., W. P. Allis, and E. S. Lamar, Phys. Rev., 48, 412 (1935)

12. Chapman, S., and T. G. Cowling, *The Mathematical Theory of Non-Uniform Gases*, 2nd Edition, Cambridge Univ. Press, 1952, esp. p. 350.

13. Wannier, G. H., Am. J. Phys., 39, 281 (1971)

14. Pitchford, L. C., and A. V. Phelps, "Comparative Calculations of Electron Swarm Properties in N_2 at Moderate E/N Values", Phys. Rev. A25, 540-554 (1982)

15. Dutton, J., "A Survey of Electron Swarm Data", J. Phys. Chem. Ref. Data, 4, 577-856 (1975)

16. Frost, L. S., and A. V. Phelps, Phys. Rev. 127, 1621-33 (1962)

17. Phelps, A. V., "Tabulations of Collision Cross Sections and Calculated Transport and Reaction Coefficients for Electron Collisions with O_2", JILA Information Center Report No. 28, September 1, 1985

18. Wadzinski, H. T., and J. R. Jasperse, "Low Energy Electron and Photon Cross Sections of O, N_2, and O_2, and Related Data", AFGL-TR-82-0008, 4 January (1982)

19. Kieffer, L. J., "A Compilation of Electron Collision Cross Section Data for Modeling Gas Discharge Lasers", JILA Information Center Report No. 13, September 30 (1973)

20. Archer, D., Mission Research Corporation, private communication.

21. Hake, R. D., and A. V. Phelps, Phys. Rev. 158, 70 (1967)